International Institute for Applied Systems Analysis
IIASA www.iiasa.ac.at

Address: IIASA, Schlossplatz 1, A-2361 Laxenburg, Austria
Email: repository@iiasa.ac.at

Working Paper **WP-24-011**

Explaining the increasing inequality in life expectancy across income groups

Miguel Sánchez-Romero (sanchez@iiasa.ac.at)
Manuel Marsicano (manuel.marsicano@oeaw.ac.at)
Michael Kuhn (kuhn@iiasa.ac.at)

Approved by

Hans Joachim Schellnhuber
Director General
14 May 2024

Table of contents

ZVR 524808900

Disclaimer, funding acknowledgment, and copyright information:
IIASA Working Papers report on research carried out at IIASA and have received only limited review. Views or opinions expressed herein do not necessarily represent those of the institute, its National Member Organizations, or other organizations supporting the work.

The authors gratefully acknowledge funding from IIASA and the National Member Organizations that support the institute (The Austrian Academy of Sciences; The Brazilian Federal Agency for Support and Evaluation of Graduate Education (CAPES); The National Natural Science Foundation of China (NSFC); The Academy of Scientific Research and Technology (ASRT), Egypt; The Finnish Committee for IIASA; The Association for the Advancement of IIASA, Germany; The Technology Information, Forecasting and Assessment Council (TIFAC), India; The Indonesian National Committee for IIASA; The Iran National Science Foundation (INSF); The Israel Committee for IIASA; The Japan Committee for IIASA; The National Research Foundation of Korea (NRF); The Mexican National Committee for IIASA; The Research Council of Norway (RCN); The Russian Academy of Sciences (RAS); Ministry of Education, Science, Research and Sport, Slovakia; The National Research Foundation (NRF), South Africa; The Swedish Research Council for Environment, Agricultural Sciences and Spatial Planning (FORMAS); The Ukrainian Academy of Sciences; The Research Councils of the UK; The National Academy of Sciences (NAS), USA; The Vietnam Academy of Science and Technology (VAST).

The authors gratefully acknowledge funding from the Austrian Science Fund (FWF) for the research project 'Life-cycle behaviour in the face of large shocks to health' (No. P 30665-G27).

This work is licensed under a Creative Commons Attribution-NonCommercial 4.0 International License**.**
For any commercial use please contact permissions@iiasa.ac.at

Explaining the increasing inequality in life expectancy across income groups*

Miguel Sánchez-Romero[1,2,3], Manuel Marsicano[1], Michael Kuhn[1,3]

[1] Wittgenstein Centre for Demography and Global Human Capital (IIASA, OeAW, University of Vienna), Vienna Institute of Demography
[2] Institute of Statistics and Mathematical Methods in Economics, TU Wien
[3] International Institute for Applied Systems Analysis, Laxenburg, Austria

May 13, 2024

Abstract

We present a novel life-cycle model, grounded in demographic principles, to examine the influence of medical progress, technological progress, and the reduction in age-independent mortality on the rise in life expectancy across socioeconomic groups. Our findings indicate that the expanding disparity in life expectancy across income groups, as well as the growing income inequality among educational groups in the US, can be attributed to a selection process that changes the composition of the initial characteristics (learning ability, schooling effort, and health frailty) of the income groups. This selection process is triggered by the rising income and medical advancements that emerged with the cardiovascular revolution in the 1970s. (JEL: D15, I12, I14, J17, J24)

1 Introduction

Over the past decades we have seen in many countries an increasing inequality not just in terms of income and wealth, but also in terms of health and life expectancy (OECD, 2017; Murtin et al., 2022). For instance, Waldron (2007) shows for the US how the gap in life expectancy at age sixty five between the top half and the bottom half of the income distribution increased monotonically from less than one year for the 1912 birth cohort to almost six years for the 1941 birth cohort. More recent data shows that this trend continues in the US, and the gap turns out to be even larger when more income groups are considered (NASEM and others, 2015). The projected gap in life expectancy between the top and the bottom one percent, for instance, is fourteen years for the 1960 birth cohort (Chetty et al., 2016).

This trend has political, economic, and social consequences. It not only poses challenges to the health sector (Frankovic and Kuhn, 2019), but also affects the public transfer system by making it more regressive, since short-lived and poorer workers end up subsidizing the pension benefits of long-lived and richer workers (Sánchez-Romero and Prskawetz, 2017; Lee and Sanchez-Romero, 2019; Sánchez-Romero et al., 2020). To derive effective policy responses that at least contain if not close the gap and mitigate its consequences, it is necessary to investigate the sources of the increasing inequality in life expectancy. Empirically,

*This project has received funding from the Austrian National Bank (OeNB) under Grant no. 18744.

there are methodological issues that complicate its study, such as reverse causality and the changing meaning of metrics on income and educational attainment over time, among others (Lee and Sanchez-Romero, 2019). To overcome these difficulties, it is necessary to assess the direction of causality between health and income and to account for how inequality is emerging over the life span of individuals, across socio-economic strata, and across cohorts over time.

To this end, we propose a novel life cycle model that accounts for frailty, in the spirit of Vaupel et al. (1979). Individuals decide about their educational attainment, consumption path, labor supply, and health investments. Given an initial health status (initial frailty level) the path of health investments determines the most likely or modal age at death. Dating back to Lexis (1879), the concept of the modal age at death has been used extensively for analyzing longevity in Demography, Actuarial Science, Statistics, and Biology. We propose using the modal age at death as a summary measure of health for several reasons. First, survival functions can be expressed in terms of the modal age at death (Horiuchi et al., 2013) and, therefore, the model generates realistic survival profiles, which are important for relevant policy analysis. Second, akin to the notion of health capital (Grossman, 1972; Fonseca et al., 2020), a higher modal age at death translates into lower mortality. Third, akin to the notion of health deficits (Dalgaard and Strulik, 2014), the modal age at death can be observed across populations and, therefore, has an empirical grounding.[1] Fourth, the modal age at death is calculated using age-specific death rates. Data on age-specific death rates are available since the invention of the life table by John Graunt in 1662 and, therefore, a wealth of data is publicly available data for its estimation. For instance, Fig. 1 shows the evolution of the modal age at death in the US from 1950 to 2019 (see red line) compared to all other countries (black dots) contained in the Human Mortality Database. Fifth, the modal age at death is a category in which individuals would "naturally" think of in terms of planning ahead, since it refers to the age to which individuals assign a high probability of dying. Last, but not least, similar to the health capital model, the modal age at death has no *a priori* upper bound, which allows individuals to invest in postponing their modal age at death as long as it is economically optimal. The fact that the health state has no upper bound, or lower bound, is a desirable feature when integrating this framework in dynamic overlapping generations models.

Within the proposed model, the disparities among individuals in terms of their education, income, life expectancy, and wealth arise from a combination of individual choices and external (childhood) circumstances that shape their demographics and economic decisions.[2] To describe the heterogeneity in childhood circumstances, we use three unobservable characteristics (endowments) – namely learning ability, effort of schooling, and the initial modal age at death – that are equally distributed across each birth cohort at the beginning of life. Differences in the initial modal age at death account for the initial heterogeneity in health. Heterogeneity in the learning ability translate into differences in labor income, while the effort of schooling enables us to accommodate the changing composition of each educational group in terms of learning ability and health across birth cohorts. Altogether, this allows us to account for the fact that with better demographic and economic conditions faced by successive birth cohort, those individuals that remain in the lower educational groups tend

[1] While health deficits are observable at the individual level, their link to survival and the modal age at death can only be established at the population level.

[2] For expositional purposes, we abstract from random health or income shocks over the lifespan of individuals. To justify this assumption, we rely on the study by Huggett et al. (2011) who show that initial heterogeneity (ability to learn, human capital, wealth at age 23) rather than random shocks explain about 61.2, 62.4 and 66.0 percent of the variation in US lifetime earnings, lifetime wealth and lifetime utility, respectively. This is consistent with earlier findings by Cunha et al. (2005) that about 60 percent of earnings variability is foreseen by agents and cannot therefore be attributed to uncertainty.

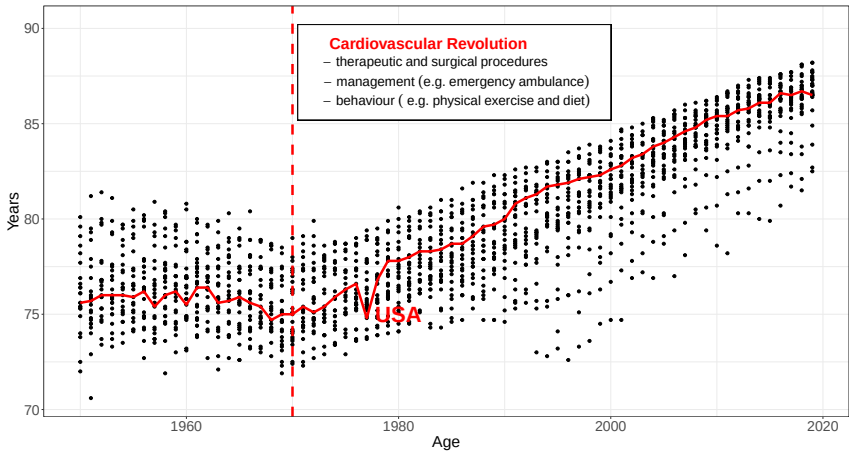

Figure 1: Modal age at death. Dots represent the modal age at death for different countries over time based on data from the Human Mortality Database (HMD). The modal age at death is estimated following Horiuchi et al. (2013).

to be more and more negatively selected.[3]

We apply the model to understand the drivers of increasing inequality in life expectancy by income. In particular, we focus on how exogenous factors, such as the reduction in age-independent mortality (e.g. from infectious diseases or accidents), productivity growth, and medical progress, influence education, income, and health outcomes across different birth cohorts. To do so, we generate results by considering a large number of random draws from the initial distribution of childhood endowments for each birth cohort (taken at twenty year intervals), by solving the life-cycle model for each of these draws, and by thus obtaining distributions of life-cycle outcomes. Then, by allowing individuals to self-select into education according to their initial endowment, we model life-cycle outcomes by educational category and income level. We calibrate the model to US data, seeking to replicate developments of key life-cycle indicators, such as life expectancy, the distribution of education over time, and the increasing gap in life expectancy by education. The model is structurally calibrated using Bayesian melding with the IMIS algorithm (Poole and Raftery, 2000), targeting US data on education, income, and mortality rates. To complete our analysis, we run counterfactual scenarios, in which we shut down each exogenous factor: reduction in age-independent mortality, productivity growth, and medical progress.

Our results show that the model is capable of replicating well the evolution of educational attainment, the distribution of income, and the death rates by education group for the US birth cohorts born in 1900, 1920, 1940, and 1960. In addition, the model is capable of matching the evolution of the life expectancy gap across income groups for the selected birth cohorts, in line with the empirical estimates of NASEM and others (2015) and Chetty et al. (2016) as well as producing realistic results for health spending and the value of life. Running counterfactual analyses, we show that medical progress, the reduction in age-independent mortality, and productivity growth have contributed positively to the increase in life expectancy for all income groups. After controlling for the initial characteristics of individuals, our model suggests that medical progress, the reduction in age-independent mortality, and productivity growth contribute almost equally to the increase in life expectancy

[3]A similar strategy has been applied by Sánchez-Romero et al. (2023) to study the impact of pension reforms across heterogeneous individuals that differ *inter alia* in terms of their life expectancy and income.

across income groups. Therefore, the model suggests that the observed increasing difference in life expectancy across income groups is due to the change in the composition of the initial characteristics, especially the initial heterogeneity in health. This result is consistent with the literature showing that the increasing gap in life expectancy is due to the lower probability of surviving ("survivability") to the ages at which individuals can benefit from the cardiovascular revolution (Dahl et al., 2024), which in our model is controlled by the initial heterogeneity in health. Furthermore, our model results are also consistent with the more classical approach that suggests that wealthier individuals invest more in health, which in turn leverages improvements in medical technology tied to these investments (Hall and Jones, 2007; Frankovic and Kuhn, 2019). These results underscore the importance of creating models capable of controlling for the selection, based on the evolution of the initial characteristics into socioeconomic groups.

The remaining sections of the paper are structured as follows: Section 2 introduces the main theoretical components of the model. Section 3 briefly explains how the initial endowments impact the optimal life cycle choices. Section 4 focuses on the calibration of the model, discussing the process of parameter determination and alignment with empirical data. Section 5 presents our findings. Section 6 summarizes and discusses future directions of research.

2 The model

We consider the life-cycle model of an individual born in year i, in which age t is modeled as a continuous variable between 0 (age 14 in real life) and T (maximum age).[4] Lifetime uncertainty is captured by the survival function $S_i(t)$, which evolves over time according to the following dynamic equation

$$\dot{S}_i(t) = -\mu_i(t, M_i(t))S_i(t). \tag{1}$$

The term $\mu_i(t, M_i(t))$ is the mortality rate of an individual born in year i, which is a function of age (t) and the modal age at death (M). The modal age at death is the most likely age at which an individual will die. This statistical measure is frequently used in demography for analyzing ageing, since it better captures mortality shifts at old age. Moreover, unlike the life expectancy or the median age at death, it is not affected by infant mortality (Horiuchi et al., 2013). To model the relationship between the mortality hazard rate and the modal age at death we follow Canudas-Romo (2008), Horiuchi et al. (2013), Missov et al. (2015), among others, and assume

$$\mu_i(t, M_i(t)) = c_{\mu,i} + be^{b(t-M_i(t))}, \tag{2}$$

where $c_{\mu,i}$ is the Makeham component for the i-th birth cohort and b is the senescence rate. The Makeham component represents the age-independent mortality (or age-independent risk of mortality), whereas the senescence rate scales the age-related mortality risk.

We assume in the following that $M_i(t)$ represents the health status of an individual born in year i at age t. At time 0 individuals are randomly endowed with an initial modal age at death $M_i(0) = M_0 \sim \mathcal{N}(\mu_M, \sigma_M^2)$, where μ_M is the average initial modal age at death across the population and where σ_M^2 is the according variance. Individuals can postpone their most likely age at death by investing $m_i(t)$, tantamount to increasing their net health-related consumption, according to the following health production function

$$\dot{M}_i(t) = A_i(E_i, t)m_i(t)^{\gamma_m}. \tag{3}$$

[4] The maximum age T can be arbitrarily high in the model.

Here, $A_i(E_i, t)$ reflects the effectiveness of health investments for an individual born in year i at age t. We follow Frankovic et al. (2020) and Skinner and Staiger (2015) by modeling medical progress, in the sense of increasing medical effectiveness, as a diffusion process[5]

$$\dot{A}_i = \begin{cases} 0 & \text{if } t < \tau_A - i, \\ g_A(E_i)(A^* - A_i) & \text{if } t \geq \tau_A - i, \end{cases} \tag{4}$$

where τ_A is the year when a new medical technology that reduces the risk of dying is introduced, and A^* is the new medical technological frontier. While Frankovic et al. (2020) and Skinner and Staiger (2015) consider diffusion at the macroeconomic level, we also follow Frankovic and Kuhn (2019) by assuming that access to state-of-the-art medicine at the individual level is depending on education. Thus, the term $g_A(E_i)$ is the inverse of the average time for an individual with educational attainment E_i to have access to the new medical technology. More educated individuals are assumed to have access sooner to the new technology than less educated individuals. The term $\gamma_m \in (0, 1)$ measures the returns-to-scale of health investments in raising the modal age at death. The fact that health can postpone the age at death by slowing down, but not reversing, the ageing process is well in line with the gradual accumulation of health deficits (Rockwood and Mitnitski, 2007; Dalgaard and Strulik, 2014). Moreover, historical data shows that the modal age at death for several countries was roughly constant before 1950 (see Fig. 1). Since we assume that the initial modal age at death is randomly assigned, the value of $M_i(t)$ reflects individual frailty at age t. In particular, given a path of health investments, individuals at age t whose $M_i(t)$ is below the average are expected to die sooner than individuals at the same age t for whom $M_i(t)$ is above average. This is an important feature of the model because it allows to combine the frailty model (Vaupel et al., 1979) with the Lee-Carter model (Lee and Carter, 1992) (see Section B in the appendix), as the two leading mortality models in the fields of Demography and Actuarial Sciences.

Preferences The expected lifetime utility of an individual born in year i at age 0, conditional on the additional years of schooling (E_i), the maximum age (T_i), the non-health-related consumption path (c_i), and the path of labor supply (ℓ_i), is given by

$$V_i(E_i, T_i, c_i, \ell_i) = \int_0^{T_i} e^{-\rho t} S_i(t) U(c_i(t), \ell_i(t)) dt - \xi_e \int_0^{E_i} e^{-\rho t} S_i(t) dt. \tag{5}$$

The first term on the right-hand side accounts for the discounted and expected stream of utility from consumption and labor (with $U(c, \ell) > 0$, $U'_c(c, \ell) > 0$, $U'_\ell(c, \ell) < 0$, $U''_{cc}(c, \ell) < 0$, $U''_{\ell\ell}(c, \ell) < 0$, and $U''_{c\ell}(c, \ell) \leq 0$). The second term reflects the expected effort of attending school (Sánchez-Romero et al., 2016; Restuccia and Vandenbroucke, 2013; Oreopoulos, 2007), which is an increasing function of the length of schooling, E_i. The parameter ρ is the subjective discount factor and $S_i(t)$ is the survival probability to age t.

Budget constraint We assume that individuals start and terminate their life course (at age T_i) without financial wealth, such that $k_i(0) = k_i(T) = 0$. To rule out adverse selection of health investments on the mortality risk premium, we assume individuals do not purchase annuities. The lifetime budget constraint then reads

$$\int_0^{T_i} (c_i(t) + m_i(t)) e^{-rt} dt = \int_{E_i}^{T_i} w_i(t) H_i(t) \ell_i(t) e^{-rt} dt, \tag{6}$$

[5]Solving Eq. (4) yields $A_i(E, t) = A^* + (A_i(E, \tau_A - i) - A^*) e^{-g(E)(i+t-\tau_A)}$ for $t \geq \tau_A - i$.

where $c_i(t)$ and $m_i(t)$ denote non-health-related consumption and health investments, respectively, and where r denotes the market interest rate. Consumption and health spending across the life course are financed by the labor income earned after the completion of schooling at age E_i. The labor income earned at age t is given by the product of labor supply, $\ell_i(t)$, age-specific productivity $H_i(t)$, and the wage rate per efficient unit of labor $w_i(t)$.

The age-specific productivity increases with schooling, following a standard Ben-Porath technology, and declines at a rate that is proportional to the mortality rate. Thus, we specify the productivity dynamics as

$$\dot{H}_i(t) = \begin{cases} \xi_h H_i(t)^{\gamma_h} - \phi\mu_i(t, M_i(t))H_i(t) & \text{for } t \leq E_i, \\ f(t, E_i)H_i(t) - \phi\mu_i(t, M_i(t))H_i(t) & \text{for } t > E_i, \end{cases} \tag{7}$$

where ξ_h denotes the innate learning ability, $\gamma_h \in (0, 1)$ denotes the returns-to-scale of education, ϕ denotes the influence of health on labor productivity, $\mu_i(t, M_i(t))$ denotes the mortality rate as a function of time and the modal age at death M_i, and $f(t, E_i)$ denotes the contribution of experience, as measured by the gap $t - E_i \geq 0$, to productivity. Note that our formulation is consistent with the literature showing that productivity declines faster for less healthy individuals (Weil, 2007; Kotschy, 2021; Bloom et al., 2024, among many others), and with the way in which early-life health and educational outcomes jointly determine mid-life health and income (Smith, 2007; van Kippersluis et al., 2010). Note here that a higher modal age at death reduces the mortality rate – see Eq. (2)– and hence positively affects the labor productivity of the individual and allows the individual to remain productive over an extended stretch of time. Furthermore, variation in the modal age at death across individuals of the same age implies variation in their productivity and in the extent to which they are able to retain productivity over their life course.

3 Optimal life cycle allocation

To understand how individuals optimal allocate their resources to postpone their modal age at death, we define three concepts: i) the value of human capital ψ_H, ii) the value of life ψ_S, and iii) the value of delaying the modal age at death ψ_M.

The value of human capital (VoHK) at age t is tantamount to the discounted value of the earnings stream over the remaining working life

$$\psi_i^H(t) := \frac{\partial V_i/\partial H_i(t)}{\partial V_i/\partial k_i(t)} H_i(t) = \int_t^{T_i} w_i(\tau)H_i(\tau)\ell_i(\tau)e^{-\int_t^\tau rds}d\tau. \tag{8}$$

As becomes evident from the human capital dynamics, see Eq. (7), individuals with a better health status (i.e. greater M_i) are better able to remain productive and enjoy a higher income, ceteris paribus their innate learning ability levels. For this reason VoHK increases with health.

The value of life (VoL) at age t is the willingness to pay for reducing the risk of dying at age t (Rosen, 1988; Costa and Kahn, 2004), which can be calculated as the marginal rate of substitution between financial wealth and the probability of survival

$$\psi_i^S(t) := \frac{\partial V_i/\partial S_i(t)}{\partial V_i/\partial k_i(t)} S_i(t) = \int_t^{T_i} \frac{U(c_i(\tau), \ell_i(\tau)) - \xi_e \mathbf{1}(t \leq E_i)}{U_c(c_i(\tau), \ell_i(\tau))} e^{-\int_t^\tau rds}d\tau. \tag{9}$$

The VoL is the monetized value of the expected utility at time t of an individual or, equivalently, the monetary value of the discounted stream of utility over the remaining life span.

Eq. (9) implies that individuals with higher human capital consume more and enjoy more leisure so that, for this reason, they are willing to pay more for reducing their risk of dying.

The value of delaying the modal at age death (VoDeM) is the willingness to pay for postponing the most likely age at which an individual will die.[6] To fully understand VoDeM, however, we draw on the earlier interpretation of the modal age at death $M_i(t)$ as a proxy for the individual's health or frailty. Notably, improvements in health allow the individual to defer mortality and, at the same time, better preserve it's human capital. Similar to VoHK and VoL, the VoDeM can be calculated as the marginal rate of substitution between the financial wealth and the modal age at death

$$\psi_i^M(t) := \frac{\partial V_i/\partial M_i(t)}{\partial V_i/\partial k_i(t)} = \int_t^{T_i} \frac{-\partial \mu_i(\tau, M_i(\tau))}{\partial M_i(\tau)} (\psi_i^H(\tau)\phi + \psi_i^S(\tau)) e^{-\int_t^\tau r ds} d\tau. \tag{10}$$

VoDeM amounts to the discounted stream of values associated with an improvement in health, as proxied by $M_i(t)$, from age t onward. This value is determined by the sum of the gains in human capital, as valued by $\psi_i^H\phi$, and survival, as valued by ψ_i^S, that are afforded through the reduction in mortality over the remaining life course that is implied by a higher $M_i(t)$.[7] According to equation (10) VoDeM is driven by two opposing forces. On the one hand, VoDeM rises with an increase in the value of human capital (ψ_i^H) and the value of life (ψ_i^S), holding age-related mortality constant. On the other hand, VoDeM declines when the age-related mortality falls, ceteris paribus ψ_i^H and ψ_i^S. Therefore, our model suggests that individuals with high incomes and poor health (measured through a low modal age at death) are the most willing to invest in health, whereas individuals with low incomes and good health are less willing to invest in health. Moreover, if two individuals have the same labor income stream along their lives, the individual with worse health will invest more (resp. less) early (resp. later) in life than the individual with better health.

3.1 Economic problem

The individual maximizes (5) by choosing the optimal path of $m_i(t)$, $c_i(t)$, $\ell_i(t)$ as well as the optimal number of (additional) years of education E_i and the maximum age T_i subject to (1)–(3), (6) and (7). The model is solved using the present value Hamiltonian (see the solution in Section A in the appendix). From the first-order conditions we obtain the optimal investment in health as

$$m_i(t) = \left(\gamma_m A_i(t) \psi_i^M(t)\right)^{\frac{1}{1-\gamma_m}}. \tag{11}$$

Eq. (11) suggests that, akin to the finding in Frankovic et al. (2020), health investments increase with medical effectiveness, A_i, and with the VoDeM (or value of health), ψ_i^M. Plugging (11) into (3) shows how the dynamics of the modal age at death depends on medical effectiveness and the value that each individual assigns to delaying the modal age at death

$$\dot{M}_i(t) = A_i(t)^{\frac{1}{1-\gamma_m}} \left(\gamma_m \psi_i^M(t)\right)^{\frac{\gamma_m}{1-\gamma_m}}. \tag{12}$$

[6] Note the conceptual difference to the expected age at death, which is the life expectancy (Canudas-Romo, 2008). In a model without mortality uncertainty, the modal age at death coincides with the life expectancy, and with the maximum age.

[7] Kuhn et al. (2015) provide a similar conceptualization of a value of health (or generalized VoL to account for the impact of health on the disutility of labor). Freiberger et al. (2024) provide a generalized value of health, taking into account the prevention of large scale health shocks and acute and chronic treatment following them.

This result has two important implications. First, it implies that increases in the value of human capital or in the value of life (hence in ψ_i^M) raise the modal age at death even when there is no change in medical effectiveness (i.e. $\dot{A}_i = 0$). Second, the contribution of a marginal increase in the value of delaying the age at death to the increase in the modal age at death is γ_m times smaller than that of a marginal increase in the state of health technology.

From the first-order conditions and the envelope conditions we obtain the laws of motion for consumption, labor, and health investments

$$\frac{\dot{c}_i(t)}{c_i(t)} = \sigma_c(t)\big(r - \rho - \mu_i(t, M_i(t))\big), \tag{13}$$

$$\frac{\dot{\ell}_i(t)}{\ell_i(t)} = \sigma_\ell(t)\left(\rho - r + \frac{\dot{w}_i(t)}{w_i(t)} + f(t, E_i) + (1-\phi)\,\mu_i(t, M_i(t))\right), \tag{14}$$

$$\frac{\dot{m}_i(t)}{m_i(t)} = \frac{1}{1-\gamma_m}\left(r + \frac{\dot{A}_i(t)}{A_i(t)} - \frac{-\dot{\psi}_i^M(t)}{\psi_i^M(t)}\right), \tag{15}$$

where $\sigma_c = -U_c/(cU_{cc})$ is the intertemporal elasticity of substitution (IES) in regard to consumption, $\sigma_\ell = U_\ell/(\ell U_{\ell\ell})$ is the IES in regard to labor. Eq. (13) is the standard Euler-condition in the absence of annuities. For $r > \rho$, the consumption path follows an inverted U-shape, with the decline setting in once the mortality hazard becomes sufficiently high. For a given lifetime income, the consumption profile will thus decline sooner for individuals with lower modal ages at death.

Eq. (14) shows how hours worked evolve over the working life according to the difference between ρ and r and the change in the wage rate, in experience, and in health, as proxied by the mortality rate. Eq. (14) implies that individuals work harder today when the interest exceeds the rate of time preference, so that they can save more today; and work harder in the future when earnings are expected to increase either because of productivity growth or growth in individual experience. The impact of mortality on labor is a priori ambiguous. On the one hand, the mortality risk reduces future consumption and leisure (since both are normal goods), and as a consequence the future labor supply increases. On the other hand, mortality is associated (through a decline in health) with an erosion of human capital, which creates an incentive to work harder today while productivity is still high. The net effect of mortality depends on the impact of health on human capital. For $\phi < 1$, individuals shift labor to older ages, while for $\phi > 1$ individuals work harder today.

Eq. (15) shows the evolution of health investments with age. Health investments tend to increase with age in line with the interest rate (i.e. individuals prefer to save today and invests the proceeds on health later in life) and in line with the rate in which personal access to effective health increases, while they decline as the value of postponing the age at death decreases. It is worth recalling that the lag in access to effective health technology tends to imply that less educated individuals respond less in terms of health utilization to improvements in the state-of-the art medicine, an effect that exacerbates an initial disadvantage (Frankovic and Kuhn, 2019). Furthermore, the value of delaying the age at death declines faster for frailer individuals. Consequently, for a given lifetime income, frailer individuals will reduce their health investments earlier so that inequality in health tends to increase over the life course both in respect to education and in respect to frailty.

The optimal educational attainment is chosen from a set of potential educational possibilities ($E_i \in \mathbf{E}$) as the argument that maximizes the expected utility (5). According to Sánchez-Romero et al. (2016), the optimal educational attainment satisfies that the returns to education exceeds the pecuniary and non-pecuniary cost of education. The pecuniary cost of education is the average return lost in the capital market due to postponing the entrance

in the labor market, whereas the non-pecuniary cost of education is determined by the ratio between the effort of schooling and the value of human capital. Noting that individuals expect to die with close to certainty before reaching the maximum age T_i, its optimal choice amounts to a "technical" closure of the model. Further details on the first order conditions can be found in Appendix A.

4 Model calibration

The model is calibrated to represent US males born in the years 1900, 1920, 1940, and 1960; i.e. $i \in \{1900, 1920, 1940, 1960\}$. The wage rate per hour worked is considered to be a function of exogenous wage rate growth (g_w), educational attainment (E_i), learning ability (ξ_h), experience ($t - E_i$), and the health status. The health status is represented by the survival probability, which in turn is a function of the modal age at death. We consider two educational groups: college and non-college. We set the educational attainment, E_i, at 4 years for non-college education, and at 8 years for college education. The returns-to-education γ_h is set at 0.66, similar to Cervellati and Sunde (2013). To estimate the returns to experience, we assume the logarithm of the wage rate can be approximated by a standard quadratic function on experience (see section D for the regression analysis). The main parameter values of the model are summarized in Table 1.

Individuals are assumed to have the following preferences:

$$U(c, \ell) = \log(c) + \alpha \frac{(1-\ell)^{1-\frac{1}{\chi}} - 1}{1 - \frac{1}{\chi}} + \bar{u}. \tag{16}$$

Consumption and leisure (i.e., $1-\ell$, when available time is normalized to one) are considered additive separable. We express the utility from consumption in logarithmic terms for consistency with balanced growth. This implies that the intertemporal elasticity of substitution on consumption σ_c is one. Leisure, rather than labor, is modeled in the utility function to account for the fact that the Frisch elasticity is increasing with age and might differ across educational groups (Keane, 2022). The term χ is the intertemporal elasticity of substitution on labor $\sigma_\ell = \chi$. The Frisch labor supply elasticity is $\chi \frac{1-\ell}{\ell}$, and $\bar{u}$ is the base level utility. Following Nishiyama and Smetters (2014), who also model heterogeneous individuals, and Keane (2022) we set the Frisch labor supply elasticity in the vicinity of 1.0 for prime age workers. Thus, we set χ at 0.5 and α at 2.67, so that prime aged individuals work 33.0 percent of their available time, which is similar to the average working hours reported by Nishiyama and Smetters (2014).

The baseline utility $\bar{u}$ is set at 6.0 to match a value of life close to \$6M for the median individual belonging to the 1960 birth cohort.[8] This parameter is important for modeling a rising health share with increases in income (Hall and Jones, 2007). The exogenous wage growth for the period 1900–2019 is based on time series data on the real hourly compensation of workers, as taken from the US Bureau of Labor Statistics and Gordon (2017). Consistent with our modeling setting, we detrended this data by the marginal impact of gains in health (proxied by the adult survival ratio) on the wage rate. The adult survival ratio in the US for the period 1933–2019 is taken from the Human Mortality Database (2024). After year 2019 we assume wages to increase at an annual rate of 0.875 percent, which is the last predicted value using a LOESS regression on our constructed time series. We set the interest rate r at 2.5 percent and the subjective discount factor ρ at 0 percent, to match the increase by age

[8] The value of $\bar{u}$ needs to be positive and sufficiently large to compensate for the negative effect on lifetime utility of the effort of schooling.

Table 1: Model parameters

	Symbol	Value	Reference
Preferences			
Base level utility	$\bar{u}$	6.0	Target: Avg. value of life of \$6M
IES on cosumption	σ_c	1.0	
IES on labor	χ	0.5	Keane (2022)
Share parameter of consumption	α	2.67	Target: Average labor supply of 33% of available time
Subjective discount factor	ρ	0.0	Lee et al. (2000) and Boucekkine et al. (2002)
Prices			
Exogenous wage rate growth	g_w	g_{wt}	US Bureau of Labor Statistics, Gordon (2017), and Human Mortality Database (2024)
Interest rate	r	2.5%	Target: Average growth rate of consumption of 1%
Initial wage rate	w	1.0	
Mortality			
Senescence rate	b	0.1000	Missov et al. (2015)
Makeham component	$\mathbf{E}[c_{\mu,1900}]$	0.003817	See equation (17)
	$\mathbf{E}[c_{\mu,1920}]$	0.001025	
	$\mathbf{E}[c_{\mu,1940}]$	0.000990	
	$\mathbf{E}[c_{\mu,1960}]$	0.000938	
Health investments			
Initial state of medical effectiveness	$A(0)$	0.15	
Final state of medical effectiveness	A^*	0.20	Fonseca et al. (2020)
Education-specific time to access state-of-the-art medicine	$g_A(E)$		Frankovic and Kuhn (2019); Frankovic et al. (2020) and Skinner and Staiger (2015)
Returns to health investments	γ_m	0.11	Target: Life expectancy at top 1% income for the 1960 birth cohort
Human capital			
Returns to education	γ_h	0.66	Cervellati and Sunde (2013)
Health impact on income	ϕ	0.848	Bloom et al. (2024)
Returns to experience	β_1	0.033959	Section D
Returns to experience-squared	β_2	-0.000533	Section D

of the cross-sectional per capita consumption profile in the US, which is close to 1 percent per year after controlling for the impact of mortality.[9]

Reduction in age-independent mortality. All birth cohorts are assumed to start with the same distribution of the initial modal age at death $\mathcal{N}(\mu_M, \sigma_M^2)$, and hence age-related mortality rates. To account for the evolution of the age-independent mortality risk, we calculate the Makeham component for each birth cohort i (i.e. $c_{\mu,i}$) using the following relationship

$$c_{\mu,i} = \mu_{30,i} - b \cdot \exp(\, b \cdot (30 - \mu_M)), \tag{17}$$

where $\mu_{30,i}$ is the observed mortality rate at age 30 for US males born in 1900, 1920, 1940, and 1960, and b is the senescence rate. We set b at 0.10, which is within the values estimated by Missov et al. (2015). The mortality rates are taken from the US Social Security Administration (Bell and Miller, 2005).

[9] In many life cycle model with survival probabilities, it is standard to assume no subjective discount factor (Lee et al., 2000; Boucekkine et al., 2002).

Medical technology. We set the elasticity of the demand for health care (γ_m) at 0.11 to match the life expectancy for the top 1 percent income group for the 1960 birth cohort as estimated by Chetty et al. (2016). In our analysis, we assume that the cardiovascular revolution sets in from the 1970s onwards (Hansen and Strulik, 2017; Ford et al., 2007). We set the initial state of the medical frontier $A(t)$ for $t < \tau_A$ at 0.15, where τ_A is the year 1970. The latest state of the medical frontier is set at 0.20 in order to replicate the increase in the average life expectancy for the cohorts born between 1900 and 1960. The value for the latest state of the medical frontier implies that the medical productivity increases at an annual rate of 0.72 percent over the period 1965 to 2005, which is the same as in Fonseca et al. (2020). Following Skinner and Staiger (2015) we set the time gap between the highly educated (vanguards) and less educated group (laggards) at 10 years. This is in line with Cutler et al. (2006) and Link and Phelan (1995) who show that higher educated individuals enjoy a health premium for their education when a new medical technology is introduced.

Impact of health on income. To parameterize the value of ϕ we follow Bloom et al. (2024) who estimate that a 1 percent increase in adult survival leads to a 1.06 percent increase in labor productivity. In our life cycle model, the estimated value from Bloom et al. (2024) is equivalent to setting ϕ at $0.848 (= 1.06 \cdot 0.8)$.[10] This value implies, according to Eq. (14), that a one percent increase in the mortality rate increases the labor supply in the next period by approximately $0.175 (\approx \chi(1-\phi) = 1.15 \cdot (1 - 0.848))$ percent, ceteris paribus all other variables. We thus find the net effect of health improvements on the intertemporal supply of labor to be small due to the offsetting impacts of a higher demand for leisure as opposed to a greater productivity. This is in line with recent findings of almost no effect of the gains in health on labor supply (Stephens Jr. and Toohey, 2022).

4.1 Bayesian melding

In addition to the standard parameters, we calibrate the initial unobservable characteristics, namely the initial modal age at death M_0, the learning ability ξ_h, and the schooling effort ξ_e, of the agents using the Bayesian melding technique with the IMIS algorithm (Poole and Raftery, 2000). The Bayesian melding provides an inferential framework for deterministic models taking into account both model's inputs and outputs. An important feature of this method is that it allows to calibrate the set of initial unobservable characteristics of the model simultaneously without facing the Borel paradox. The (unconditional) distributions of these characteristics are fixed across birth cohorts. The fixation of the characteristics across all birth cohorts allows us to observe compositional changes taking into account selection effects (Sánchez-Romero et al., 2023). We provide the details of the Bayesian melding calculations in Section E.

Marginal posterior distribution of characteristics We define θ as a set of inputs, consisting of the mean and the standard deviation of the modal age at death, of the learning ability level, and of the effort of schooling, and the absolute value of the correlation between the learning ability and the effort of schooling and calibrate randomly drawn input sets in a way that best matches the life-cycle outcomes observed in the data. Using the calibrated

[10] Note that Bloom et al. (2024) regress the logarithm of labor productivity to adult survival, which is defined as the probability of surviving to age 65 conditional on being alive at age 15 (i.e. $S(65)/S(15)$). Given that in our model setup, the logarithm of labor productivity is proportional to the logarithm of adult survival, we need to multiply the estimated coefficient 1.06 from Bloom et al. (2024) by the average adult survival in their sample, which is 0.80.

input-sets θ shown in Figure 10 in Appendix E, we generate the marginal posterior distribution of the characteristics (i.e. the initial modal age at death, learning ability level, and effort of schooling). Figure 2 is obtained after drawing a sample of 15 000 sets of individual characteristics for each of the 200 random combinations of input-sets θ. These characteristics are assumed to be constant across cohorts. This implies that while the unconditional distribution of the characteristics is the same across cohorts, the conditional distribution of the characteristics by socioeconomic group, specifically by education, may vary across birth cohorts, allowing us to control for selection effects into specific socioeconomic (SE) groups, in our case education. In the results section, we will use income as our SE variable, given that mortality by income level has not been used in the calibration process.

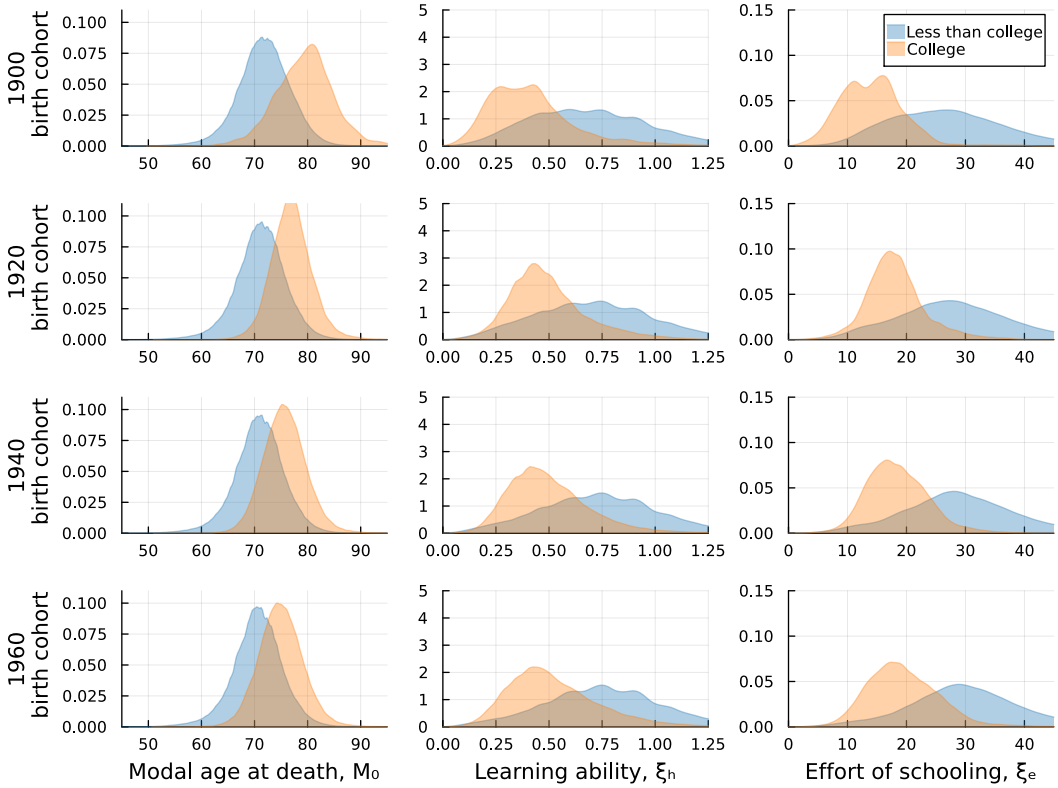

Figure 2: Conditional marginal posterior distributions of individuals' characteristics on educational attainment: selected birth cohorts (1900, 1920, 1940, 1960). The first column on the left shows the distribution of the initial modal age at death (M_0), the second column is the distribution of the learning ability level (ξ_h), and the last column on the right is the distribution of the effort of schooling (ξ_e). The characteristics of individuals with less than college are represented in blue, while the individuals with college education are represented in orange.

Figure 2 illustrates how the distributions of the characteristics for each educational group change across birth cohorts. The upper panels show that college educated individuals born in 1900 had on average a higher modal age at death, a lower learning ability, but also a lower schooling effort than individuals with less than college education. As we move to more recent birth cohorts (see bottom panels), the figure shows a convergence between the two educational groups in terms of learning ability and schooling effort. As a consequence, the

learning ability of non-college educated individuals belonging to the 1960 birth cohort is on average lower than of non-college educated individuals born in 1900. Therefore, the calibration shows that individuals with less than college are becoming more negatively selected. Similar patterns are being obtained for Austria in Sánchez-Romero et al. (2023), without considering health as an unobservable characteristic.

Model fit Figure 3 shows the fit of the model to education, demographic, and economic data for selected birth cohorts. The figure is divided into eleven panels. The top panels are devoted to education data (Panel A) and to the distribution of the wage rate at age 40 by education group (Panels B and C). The middle panels depict cohort age-specific mortality rates (in logs) for the selected birth cohorts (Panels D–G). The bottom panels show the age-specific mortality rates (in logs) by education group for the 1940 birth cohort (Panels H and I) and for the 1960 birth cohort (Panels J and K). Figure 3 shows that the model is capable of replicating sufficiently well education, demographic, and economic data, even if Panel A illustrates that the model tends to underestimate the proportion of individuals achieving college education compared to the actual data. Moreover, it should be observed that the age-specific mortality rates generated by the model deviate slightly from the recorded mortality rates for ages 80 and above. However, this is not of deep concern since most of the data for the ages above 80 are still unknown and are based on extrapolations.

4.2 Cross-validation: Evolution of life expectancy by income across birth cohorts

Our model is capable of endogenously generating realistic age-specific mortality rates that differ by socioeconomic group and birth cohort. To validate our simulation results on the evolution of mortality, Figure 4 shows a comparison between our estimated life expectancy at age fifty for males born in 1920 and 1940 by wage quintile (violet and yellow bars) and the estimated life expectancy at age fifty for males born in 1930 (green bars), taken from the Committee on the Long-Run Macroeconomic Effects of the Aging U.S. Population (NASEM and others, 2015). We choose the data on males born in 1930, rather than in 1960, because the mortality data on males born in 1930 relies less on extrapolations. Figure 4 shows that our model is capable of generating a realistic life expectancy at age fifty by income quintile, since the estimates for males born in 1930 by income quintile lie between the values we estimate for the neighbouring 1920 and 1940 cohorts.

To complement the previous validation, Figure 5 shows the expected age at death for forty-year old men born in 1900, 1920, 1940, and 1960 by wage rate percentile simulated by the model. This figure shows a positive relationship between the wage rate percentile and the expected age at death for all birth cohorts, which becomes stronger for the most recent ones. The difference in the expected age at death for forty-year old men between the 5th and 95th percentile groups is close to $2.0 (= 73.9 - 71.9)$ years for the 1900 birth cohort, while this difference is $10.8 (= 86.0 - 75.2)$ years for the 1960 birth cohort. Comparing the red dots to the blue dots shows that the model is capable of generating differences in expected age at death by income that are consistent in shape with recent cross-sectional death rate estimates for the US (Chetty et al., 2016). This is important because the model has not been calibrated to target this data, which therefore cross-validates the model results.

In addition, Figure 5 shows that the widening difference in life expectancy across income groups is the result of a slow increase in life expectancy between the 1900 and 1960 birth cohorts for the lowest percentile groups (3.3 years for the 5th percentile group) as compared to the highest percentile groups (12.1 years for the 95th percentile group). In other words,

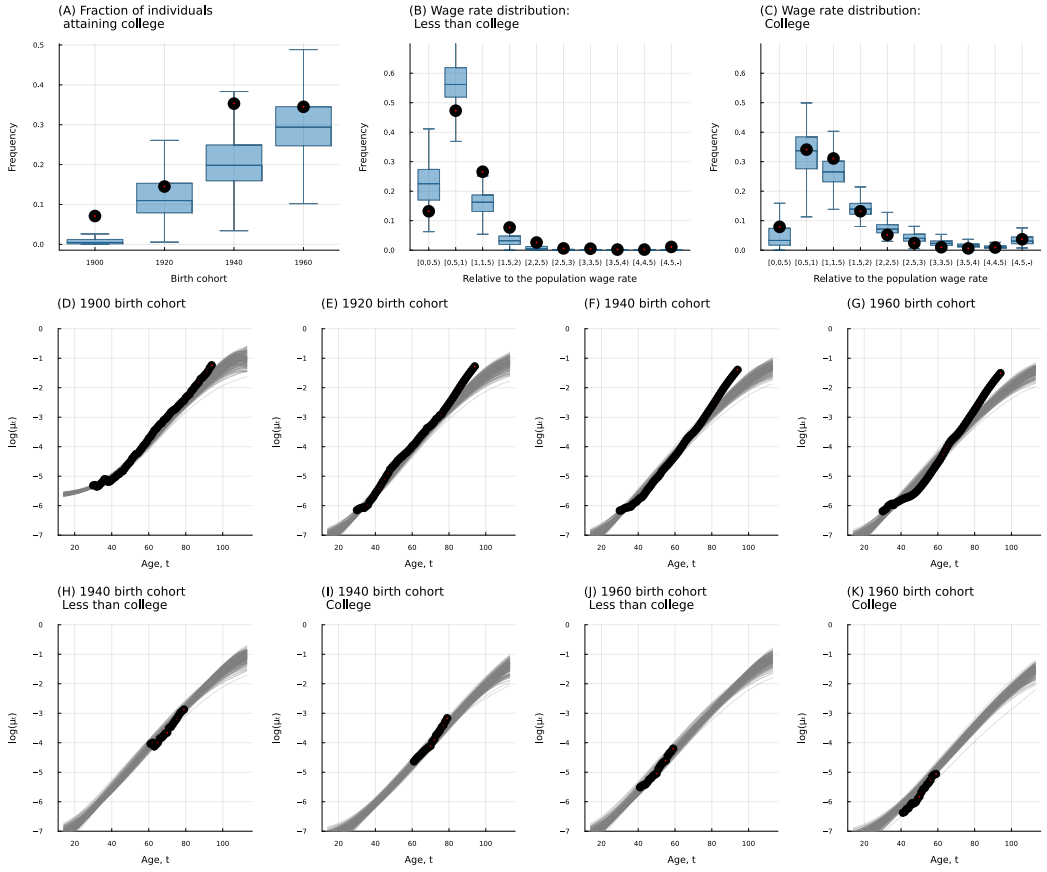

Figure 3: Model fit.

Notes: Black-red dots depict actual data on education, on the wage rate distribution for college and non-college educated workers between ages 40-44 in year 2000, on death rates for each birth cohort, and on mortality rates for college and less than college individuals belonging to the 1940 and 1960 birth cohorts. Source: Data on educational attainment by birth cohort is taken from Goujon et al. (2016); cohort data on age-specific mortality rates by birth cohort have been collected from the US Social Security Administration (Bell and Miller, 2005). Cohort age-specific mortality rates by educational attainment have been calculated using data from CDC (Mortality Multiple Cause Files). See the details of the estimations in appendix C. The wage rate per hour worked for college and non-college educated individuals aged 40-44 in the year 2000 is taken from IPUMS-CPS data and controlled for race, occupation, industry, and state.

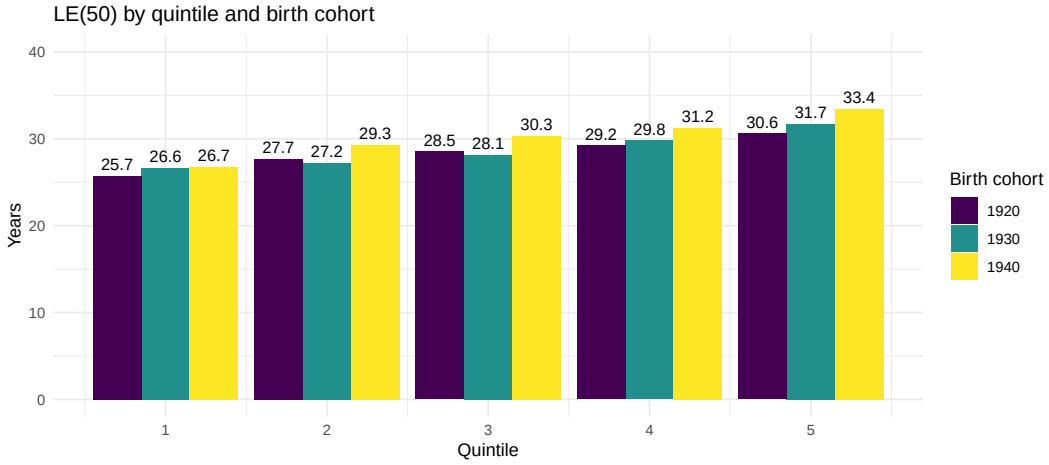

Figure 4: Estimated life expectancy at age fifty for US males born in 1920, 1930, and 1940, by income quintile. *Source: Data for 1920 and 1940 is generated with the life cycle model. Data for 1930 comes from NASEM and others (2015), which was estimated using Health and Retirement Study data.*

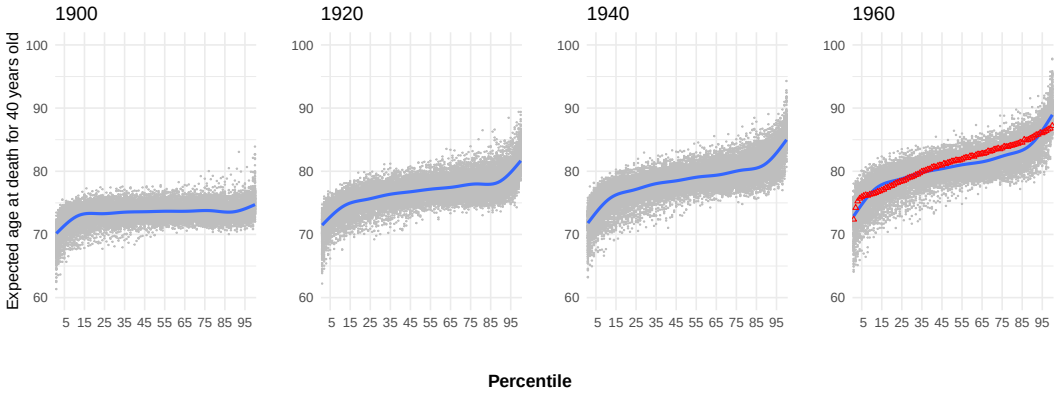

Figure 5: Expected age at death for forty-year old US males born in 1900, 1920, 1940, and 1960 by wage rate percentile (age group 40-44). Notes: Gray dots depict the mean expected age at death in each percentile group for the $N_\theta = 200$ randomly drawn sets of model inputs. The blue line is the average value for each percentile group across all the randomly drawn sets of model inputs. The red triangles correspond to the estimated race- and ethnicity-adjusted life expectancy for forty-year old men by household income percentile, 2001–2014 from Bergeron et al. (2022).

the years of life gained at age forty per decade are 0.55 and 2.02 for the 5th and 95th percentile group, respectively. In the next subsection, we focus on explaining the divergence in the years gained.

5 Simulation results

In this section, we use the model to clarify the causes of the increasing mortality gap across socioeconomic groups. This topic is related to a large body of literature that seeks to understand the causes of the overall mortality decline (Cutler et al., 2006). We divide this section into three subsections. First, we employ the model results to study (optimal) health investments across the different socioeconomic groups. Recall that health investments have a positive effect on the modal age at death and hence on life expectancy. Second, we assess the factors that have contributed to the evolution of life expectancy across birth cohorts. And third, we assess the factors that have contributed to the increasing life expectancy gap across socioeconomic groups in terms of income and education.

To produce the results, we have randomly drawn $N_\theta = 200$ sets of inputs $(\theta_1, \theta_2, \ldots, \theta_{N_\theta})$ from the posterior distribution of the initial characteristics (see Figure 10). For each input-set θ_j, $j \in \{1, \ldots, N_\theta\}$, we have generated $n = 15\,000$ sets of individuals' initial characteristics and solved their life cycle model. Then, for each θ_j input-set, we select out of the $n = 15\,000$ initial sets of characteristics those that are found in the four birth cohorts and in all the counterfactual simulations to be analyzed. This step reduces the average sample size of sets of characteristics per θ_j input-set to $n = 94$. Hence, the average sample size per simulation across the four birth cohorts is 74 844 individuals. In the following, we denote by $\mathcal{Z}|\theta$ the set of all potential combinations of initial characteristics given the input-set θ, while $\zeta = (M_0, \xi_h, \xi_e) \in \mathcal{Z}|\theta$ represents the ternary of initial characteristics of an individual within the set $\mathcal{Z}|\theta$.

To represent different socioeconomic groups, we stratify our sample by wage quintile groups. We choose the wage rate, instead of labor income, for two reasons. First, wage rate data has been used for calibrating the model, and therefore this variable is consistent with actual data (see Figure 3). Second, labor income depends not only on the wage rate but also on labor supply, and hence labor income is less stable than the wage rate. Similarly, for comparison across individuals within the same birth cohort, we choose age forty as our reference age group.

5.1 Health investments

We now proceed to study the health investments of our heterogeneous individuals. Table 2 reports the mean values of the set of initial characteristics, labor income at age forty, the health investment at age forty, the effective value of reducing mortality at age forty, and the value of life at age forty by wage quintile and birth cohort (only 1900 and 1960 birth cohorts). Notice that to report the mean values for each birth cohort of any economic or demographic variable x, when not all individuals face the same a priori survival probability, it is necessary to apply the following formula:

$$x_q(t) = \sum_{j=1}^{N_\theta} \frac{1}{N_\theta} \left(\int_{\mathcal{Z}|\theta_j,q} \frac{S(t,\zeta)}{S_{\theta_i,q}(t)} x(t,\zeta) d\,\mathrm{P}(\zeta) \right)$$

with

$$S_{\theta_j,q}(t) = \int_{\mathcal{Z}|\theta_j,q} S(t,\zeta) d\,\mathrm{P}(\zeta),$$

where q represents the income quintile, where $\mathcal{Z}|\theta_j, q$ is the set of initial characteristics given the input set θ_j for income quintile q, and where the ratio of survival probabilities is a weight that reflects the odds that an individual at age t with initial characteristics ζ is observed

relative to the average individual of the same age within the group. The term $\mathrm{P}(\cdot)$ is the cumulative distribution function of $\mathcal{Z}|\theta_j, q$.

Table 2 is divided into two panels. The upper panel shows the mean values for the 1900 birth cohort, while the bottom panel does so for the 1960 birth cohort. Each panel starts by reporting the life expectancy at age forty and the mean initial characteristics (modal age at death, learning ability, and effort of schooling) for each wage quintile of the respective birth cohort. The table subsequently presents the fraction of individuals who attain college education and the mean labor income. Note that all mean income values are expressed in dollars of year 2000. Finally, the panel shows the shares of health investments in labor income, the value of delaying the modal age at death, and the value of life for each wage quintile.

Table 2: Mean values at age forty for the main economic variables of the baseline model by wage quintile and birth cohort (in 2000 US dollars)

		wage quintile				
		1st (lowest)	2nd	3rd	4th	5th (highest)
Birth cohort: 1900						
Life expectancy at age 40	LE(40)	28.60	31.34	32.51	32.74	32.36
Initial characteristics						
Initial modal age at death	M_0	67.40	70.10	71.20	71.16	70.49
Learning ability	ξ_h	0.28	0.38	0.46	0.56	0.73
Effort of schooling	ξ_e	11.87	15.66	18.54	22.41	29.22
College share (in %)		0.32	0.06	0.12	0.24	0.82
Labor income	$y = wH\ell$	\$3.58K	\$4.78K	\$5.90K	\$7.52K	\$10.94K
Health investment share	m/y (in %)	5.95	6.46	6.87	7.31	8.21
Value of delaying modal age at death (VoDeM)	ψ^M	\$15.21K	\$21.78K	\$27.73K	\$36.29K	\$54.19K
Value of life (VoL)	ψ^S	\$0.42M	\$0.65M	\$0.85M	\$1.11M	\$1.62M
Birth cohort: 1960						
Life expectancy at age 40	LE(40)	31.14	35.28	38.75	41.35	44.59
Initial characteristics						
Initial modal age at death	M_0	64.93	67.96	70.50	72.28	74.16
Learning ability	ξ_h	0.33	0.45	0.50	0.54	0.60
Effort of schooling	ξ_e	14.11	18.96	20.64	21.89	23.15
College share (in %)		13.75	27.04	44.16	58.72	78.92
Labor income	$y = wH\ell$	\$17.97K	\$28.15K	\$37.31K	\$48.59K	\$75.42K
Health investment share (in %)	m/y	10.55	11.57	12.28	13.00	14.30
Value of delaying modal age at death (VoDeM)	ψ^M	\$80.94K	\$136.83K	\$184.01K	\$242.01K	\$369.18K
Value of life (VoL)	ψ^S	\$2.24M	\$4.09M	\$5.79M	\$7.84M	\$12.36M

Note: We take as the reference income \$37 339, which is the median value of earnings of male full-time, year-round workers in the US in year 2000, see Money Income in the US 2000 (U.S. Census Bureau, 2001).

Table 2 shows in the top panel that for the 1900 birth cohort the life expectancy at forty for the highest quintile group (32.36 years) exceeds the life expectancy for the lowest quintile group (28.60 years) by some 3.76 years. For the 1960 birth cohort, the gap in life expectancy at age forty between the highest and the lowest quintile groups has increased to 13.45 ($= 44.59 - 31.14$) years. As will be shown, the increasing gap in life expectancy is partly driven by health investments and partly by the change in the initial characteristics across the socioeconomic groups. While life expectancy is strictly increasing with income along the quintiles for both birth cohorts, Table 2 shows that in respect to the mean initial

modal age at death, this only holds clearly for the 1960 birth cohort, showing a difference of 9.23 (= 74.16 − 64.93) years between the highest and lowest quintile; whereas for the 1900 cohort the difference in the mean initial modal age at death between the highest and the lowest quintile is 3.09 (= 70.49 − 67.40) years. Comparison across the birth cohorts then shows that while the initial modal age at death has for the 1960 cohort increased by some 3.67 (= 74.16 − 70.49) years for the highest quintile, it has actually declined by some −2.47 (= 64.93 − 67.40) years for the lowest quintile. Recall that the unconditional distribution of characteristics is the same across birth cohorts. Therefore, the results suggest that the increasing gap in life expectancy is partly driven by a process of selection on health into the income groups.

In contrast to the evolution in the modal age at death, Table 2 shows a process of convergence in the learning ability and in the effort of schooling between the two extreme quintile groups for the more recent birth cohorts. The difference in the average learning ability between the 5th and 1st quintile groups declined from 0.45 (= 0.73 − 0.28) for the 1900 birth cohort to 0.27 (= 0.60 − 0.33) for the 1960 birth cohort. Similarly, the effort of schooling between the 5th and 1st quintile groups declined from 17.35 (= 29.22 − 11.87) for the 1900 birth cohort to 9.04 (= 23.15 − 14.11) for the 1960 birth cohort. This implies that the increasing inequality across income groups is due to selection on the (unobservable) initial health characteristics at age fourteen rather than learning ability or schooling effort.

Another interesting result can be seen when comparing labor income between the 5th and 1st quintile groups for the two birth cohorts. In the top panel of Table 2, we can see for the 1900 birth cohort that at age forty the highest quintile earns close to 3.06 (= $\$10.94K/\$3.58K$) times more than the lowest quintile. This ratio is close to 4.20 (= $\$75.42K/\$17.97K$) for the 1960 birth cohort. According to our model assumptions, the increasing gap in labor income across quintiles is due to changes in human capital (H_i) and in labor supply (ℓ_i), since the rate of increase in hourly wages per unit of human capital is assumed to be the same for all individuals.[11] Individuals with better health conditions (i.e. a higher average M) face lower declines in their productivity and benefit from higher human capital. Since labor supply is positively affected by human capital, they also supply more intensive labor (hours worked).

The last section of each panel in Table 2 shows for each quintile group the income share of health investments (m_i/y_i), as well as the value of delaying the modal age at death (ψ_i^M), and the value of life (ψ_i^S). Similar to Hall and Jones (2007) and Frankovic et al. (2020), the income share of health investments (i.e. m_i/y_i) is increasing in income. For instance, between the 1960 and 1900 birth cohort labor income of the 3rd quintile group increased by 632%(= $\$37.31/\$5.90 \times 100$), while health spending increased by 1 130% (= $632 \times 12.28/6.87$). Note that the increase in health spending is higher for the 5th quintile group (1 201% = $(75.42/10.94) \times (14.30/8.21) \times 100$) compared to 1st quintile group (890% = $(17.97/3.58) \times (10.55/5.95) \times 100$). Altogether, the increase in the health share over time is reflecting that health and longevity are superior goods,[12] while concomitant medical progress maintains the effectiveness of health investments.

Looking at the value of delaying the modal age at death, or by proxy, the value of health, suggests that the increase in health spending is driven by both the rise in labor income and

[11] Despite our assumption about the same hourly wage rate per unit of human capital, our model generates a higher increase in the wage rate (incl. human capital) for individuals belonging to the highest income quintile and with college education. This is because of the increasing and positive correlation for the most recent birth cohorts with respect to learning ability and educational attainment by wage quintile.

[12] While the marginal utility of consumption tends to decline for a given lifetime as individuals grow richer, additional life years in good health tend to increase in value. One important factor in this is the positive base level of utility.

medical progress. This is easily seen by dividing the value of delaying the modal age at death by labor income, which shows that this ratio is stable and ranges between 4.2 and 5.0 across income groups in both birth cohorts. Thus, if we divide and multiply ψ_i^M by labor income (y_i) in Eq. (11) and rearrange terms, we can write health spending as

$$m_i(t) = (A_i(t)y_i(t))^{\frac{1}{1-\gamma_m}} \left(\gamma_m(\psi_i^M(t)/y_i(t))\right)^{\frac{1}{1-\gamma_m}},$$

where the second term in parenthesis on the right-hand side is quite stable over time. Thus we see that for a constant $\psi_i^M(t)/y_i(t)$, health investments $m_i(t)$ increase in both the state of medicine $A_i(t)$ and income $y_i(t)$. In the next section, we assess the contribution of each factor to the increase in life expectancy.

The last row of each panel in Table 2 shows that the model generates values of life (VoL) that are within those reported in the literature Costa and Kahn (2004) and Aldy and Viscusi (2008). For instance, provided that the average annual income for US male full-time workers in the year 2000 was \$37 339 U.S. Census Bureau (2001), Table 2 implies an average VoL of \$5.79 millions for the 3rd quintile in the 1960 birth cohort. Similarly we have that the VoL for the 1960 birth cohort ranges between \$2.24 millions for the 1st quintile and \$12.36 millions for the 5th quintile. The VoL for the 1900 birth cohort ranges between \$0.42 millions for the 1st quintile and \$1.62 millions for the 5th quintile. The VoL for the 3rd quintile is 0.85 millions, which is also close to the \$1.36 millions estimated by Costa and Kahn (2004) in year 1940 for cohorts born between 1895 and 1909.

5.2 Contributions to the increasing life expectancy across birth cohorts

The model contains four exogenous factors, which are modeled as independent processes: i) medical progress (F1), ii) the reduction in age-independent mortality (F2), e.g. through the the prevention or treatment of infectious diseases and improved safety, iii) the rise in the effective wage rate per hour worked (F3), and iv) the timing of the cardiovascular revolution in relation to the educational pathways amongst the population (F4), determining the extent of access to state-of-the-art medicine (see section 4).

To assess the contribution of each exogenous factor to the increase in life expectancy from the 1900 birth cohort to the 1960 birth cohort, we run counterfactual analyses in which we shut down each of the exogenous factors in the model. In the first counterfactual experiment, we assume that the medical progress, denoted by A_i, remains constant at the level before year 1970, rather than assuming that it gradually increases from 0.15 to 0.20 after 1970, as in the baseline. This assumption will imply a reduction in the return to health investments, which will negatively impact on the increase in the modal age at death and hence on life expectancy, ceteris paribus health investments. Following a similar strategy, in the second counterfactual, we assume no reduction in the age-independent mortality. Thus, we consider that the estimated $c_{\mu,1900}$ for the 1900 birth cohort is also applied for all the remaining birth cohorts. This assumption will imply a lower life expectancy for all individuals, ceteris paribus their health investments. In the third counterfactual experiment, it is assumed that wage rates per unit of human capital do not increase over time. In contrast to the baseline, in which it is assumed that all wage rates per unit of human capital increase at an exogenous rate of g_{wt}, based on data from US Bureau of Labor Statistics and Gordon (2017). Thus, the share of health investments will diminish given the reduction in lifetime income as health and longevity are superior goods (Hall and Jones, 2007), and hence the life expectancy of individuals is expected to decline. Finally, in the fourth counterfactual, it is assumed that fifty percent of individuals from both educational groups benefit from the cardiovascular

revolution after 10 years, whereas in the baseline model, it is assumed that fifty percent of individuals with college education have access within 5 years to the new medical frontier, while it takes 15 years for individuals without college education. The counterfactual thus implies a faster increase in life expectancy for the less educated individuals and a reduction in life expectancy for the highest educated relative to the baseline.

To assess the contribution of each exogenous factor to the increase in life expectancy across birth cohorts, we first calculate the average increase in life expectancy between each birth cohort and the 1900 birth cohort for each counterfactual scenario; i.e. $\text{LE}_i^k - \text{LE}_{1900}^k$ for $k \in \{\text{B, F1, F2, F3, F4}\}$ and $i \in \{1900, \ldots, 1960\}$. Second, we calculate the impact on life expectancy of the k-th factor for the i-th birth cohort as the difference of $\text{LE}_i^k - \text{LE}_{1900}^k$ between the baseline and the counterfactual associated to the k-th factor, $I_i^k = (\text{LE}_i^B - \text{LE}_{1900}^B) - (\text{LE}_i^k - \text{LE}_{1900}^k)$. However, since the life cycle model is not a linear model, the sum of the impacts for a given birth cohort of all exogenous factors is not necessarily equal to the increase in life expectancy in the baseline for that birth cohort. Therefore, we compute the contribution of factor k to the increase in life expectancy for the i-th birth cohort as follows

$$C_i^k = (\text{LE}_i^B - \text{LE}_{1900}^B)\frac{I_i^k}{\sum_n I_i^k} \text{ for all } k \in \{\text{F1, F2, F3, F4}\}. \tag{18}$$

Figure 6 shows the total number of years-gained in life expectancy at age forty for US males born in 1920, 1940, and 1960 relative to the life expectancy at age forty for US males born in 1900. The model generates an average total number of years gained relative to the 1900 birth cohort of 3.24 for the 1920 birth cohort, of 5.00 for the 1940 birth cohort, and of 6.86 years for the 1960 birth cohort. Thus, our results suggest an average annual increase in life expectancy at age forty of 0.162 years for cohorts born between 1900 and 1920 and of 0.114 years for cohorts born between 1920 and 1960. Note that our numbers are reasonably close to Bell and Miller (2005), who project an increase in life expectancy at age forty of 2.63 for the 1920 birth cohort, 5.43 for the 1940 birth cohort, and 7.13 for the 1960 birth cohort compared to the life expectancy at age forty for the 1900 birth cohort.

Figure 6 also provides information on the estimated contribution of each exogenous factor to the total number of years gained. Dark violet shows the total and relative contribution of the wage increase to the overall years gained (see the white numbers), turquoise indicates the contribution of the reduction in age-independent mortality, green represents the contribution of medical technological progress, and yellow shows the contribution of educational differences in the access to the medical improvements from the cardiovascular revolution. Figure 6 reveals three major drivers of the increase in the additional years of life: i) the rise in the wage rate per unit of human capital, ii) medical progress, and iii) the reduction in age-independent mortality. The model suggests that all three factors have a fairly similar contribution to the increase in life expectancy at age forty, although their importance varies across cohorts. For the 1920 birth cohort, the most important factor is the increase in the wage rate (40 percent of the total increase), followed by the reduction in age-independent mortality (30 percent). For the 1960 birth cohort, the most important factor is medical progress (35 percent), followed by the reduction in age-independent mortality (34 percent). These numbers are in line with Hall and Jones (2007), who estimate that 35 percent of the reduction in mortality is due to technological change. However, our estimates are lower than those of Fonseca et al. (2020), who estimate that medical technology may explain around 50 percent of the increase in life expectancy over the period 1965-2005.[13]

[13]We report in Table 4 in appendix F the contribution of the four factors to the increase in life expectancy from the 1900 birth cohort at different ages. Table 4 shows that the relative contributions of each factor to the increase in life expectancy at ages 15, 40, and 65 are quite similar. Intuitively, the contribution of

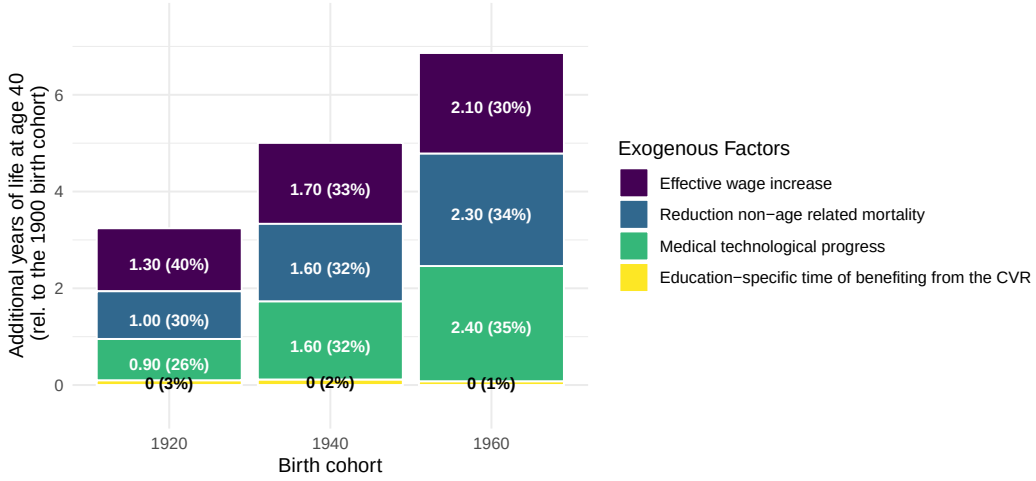

Figure 6: Contribution of exogenous factors to the increase in life expectancy at age 40 from the 1900 to 1960 birth cohorts.

5.3 Contribution to the increasing gap in life expectancy across income groups

The model also allows to assess the extent to which the exogenous factors have contributed to the increase in life expectancy across income quintile groups. However, since the initial unobservable characteristics (i.e. initial modal at age death, learning ability, and effort of schooling) of individuals belonging to the different quintile groups vary endogenously across cohorts, our assessment could be biased. To avoid biasing our estimates due to the compositional change, we rearrange our database using a matching process. First, we have identified the initial unobservable characteristics of individuals belonging to the different income quintiles for the 1960 birth cohort. Second, we identify the individuals that belong to the 1900 birth cohort who have the same initial unobservable characteristics as those in the 1960 birth cohort. This strategy rules out any bias, since the unobservable characteristics are the same. Of course, these two steps can only be done because all the results are model generated.

Using the simulated results, Figure 7 shows the frequency at which a set of unobservable characteristics from quintile $u \in \{q_1, q_2, q_3, q_4, q_5\}$ for the 1900 birth cohort is represented in quintile $v \in \{q_1, q_2, q_3, q_4, q_5\}$ for the 1960 birth cohort. There are three important highlights in Figure 7. First, over sixty percent of individuals with a specific set of initial (unobservable) characteristics from the bottom quintile for the 1900 birth cohort are also selected into the bottom quintile for the 1960 birth cohort. This finding suggests that individuals with these initial (unobservable) characteristics face significant challenges in moving to higher income quintile groups, despite the advancements in the exogenous factors (i.e. the increase in wages, medical progress, reduction in age-independent mortality). Second, the observation that the frequencies for the 2-4 quintile groups on the main diagonal are small compared to those outside suggests significant mobility of characteristics across the intermediate income

the increase in wage rates is slightly higher at younger ages than at older ages, whereas the contribution of medical progress is slightly lower at younger ages than at older ages.

quintiles from the 1900 to the 1960 birth cohorts. Indeed, the higher frequencies in the top right corner indicate that individuals with more favorable initial characteristics in the 1900 birth cohort tend to be more represented in higher quintiles in the 1960 birth cohort. This pattern reveals a strong selection to the detriment of individuals with unfavourable characteristics as well as the increasing life expectancy gap across income groups for the 1960 birth cohort.

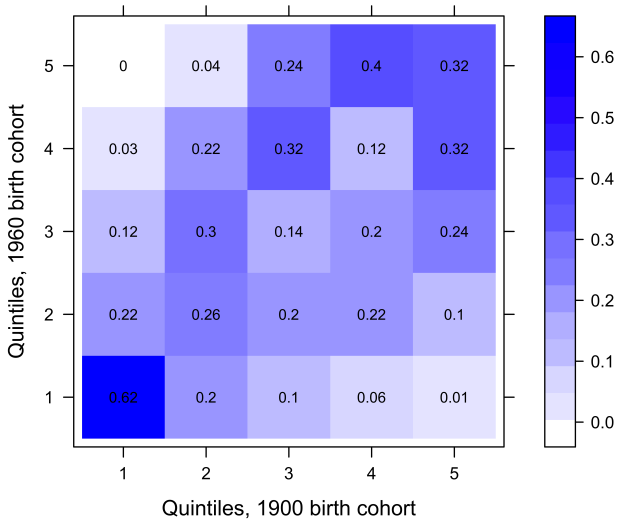

Figure 7: Frequency of initial (unobservable) characteristics across wage quintile groups for the 1900 and 1960 birth cohorts. Note: See the average initial characteristics within each cell in Fig. 13 in appendix H.

To calculate the contribution of each exogenous factor $k \in$ {F1, F2, F3, F4} on the increase in life expectancy from the 1900 birth cohort to the i-th birth cohort for the q-th income quintile, we apply the following formula

$$C_{iq}^{k} = (\text{LE}_{iq}^{\text{B}} - \text{LE}_{1900,q}^{\text{B}}) \frac{I_{iq}^{k}}{\sum_{n} I_{iq}^{k}}, \tag{19}$$

where $I_{iq}^{k} = (\text{LE}_{iq}^{\text{B}} - \text{LE}_{1900,q}^{\text{B}}) - (\text{LE}_{iq}^{k} - \text{LE}_{1900,q}^{k})$ is the impact of the k-th factor on the life expectancy of individuals were born in year i and belong to the q-th quintile group.

Figure 8 illustrates the estimated contribution of each exogenous factor to the increase in life expectancy at age forty between US males born in 1900 and 1960 by wage quintile. The figure shows four main findings. First, all exogenous factors have contributed to widening the difference in life expectancy between the 1st and the 5th quintile. In absolute terms, the exogenous factors account for a total increase in life expectancy of $4.6 (= 1.4 + 1.7 + 1.7 - 0.2)$ years for individuals in the lowest quintile and of $9.1 (= 2.7 + 3.0 + 2.9 + 0.5)$ years for individuals in the top quintile. Therefore, when comparing the life expectancy between US males born in 1900 and 1960, our model suggests that the individuals belonging to the top

quintile group have gained on average $4.5(= 9.1 - 4.6)$ years more of life than those belonging to the bottom quintile, after controlling for compositional changes. The rationale for this result is that individuals who earn more, proportionally allocate a higher fraction of their income to health investments, which allow them to postpone their age of death. Notably, these investments are leveraged by concomitant medical progress, similar to what has been demonstrated by Frankovic and Kuhn (2019). Comparing the results in Figure 8 to Table 2 provides information on the influence of compositional changes on the increase in life expectancy across income groups. Table 2 suggests that those individuals belonging to the top quintile group have gained on average $9.69(= (44.59 - 32.36) - (31.14 - 28.60))$ years more of life than those belonging to the bottom quintile, without controlling for compositional changes (see Figure 12 in appendix F for a comparison between the controlled and uncontrolled experiments on the contribution of factors to the increasing gap in longevity). Thus, compositional changes in the initial (unobservable) characteristics across income groups, which are also influenced by exogenous factors, explain fifty-three percent $(1 - 4.5/9.69)$ of the observed increase in the longevity gap between the bottom and top quintiles.

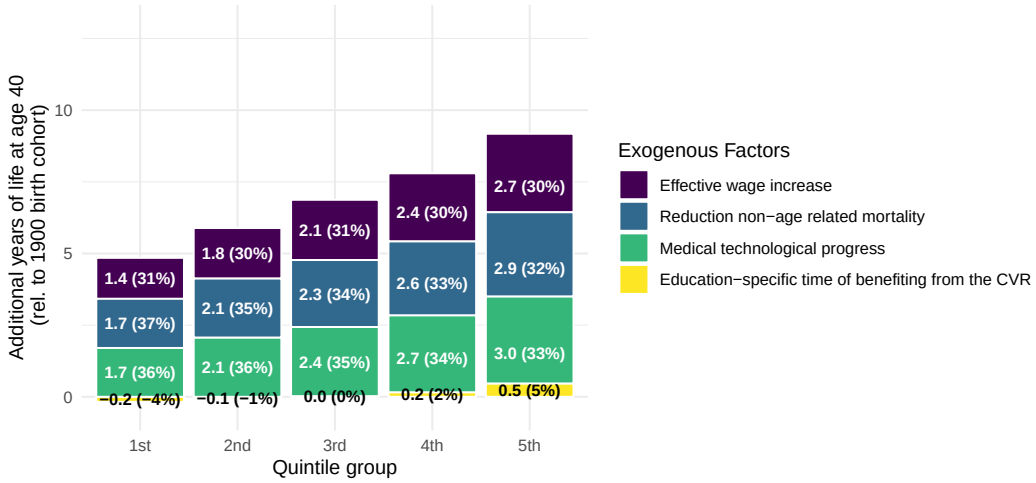

Figure 8: Contribution of exogenous factors to the increase in life expectancy at age 40 from the 1900 to 1960 birth cohorts by wage quintile.

Second, the reduction in age-independent mortality has benefited all income groups. This is because lower mortality rates positively affect labor productivity —see Eq. (7), raising lifetime income and lifetime consumption. As a result, individuals invest more in health because they value more their human capital and survival. The number of years-gained through the reduction in age-independent mortality are much larger for individuals in the highest quintile (2.9 years) than for individuals in the lowest quintile (1.7 years). Hence, this factor explains a difference of $1.2(= 2.9 - 1.7)$ years out of the total of 4.5 years (or twenty-seven percent), after controlling for compositional changes in the initial characteristics. For the uncontrolled case, the reduction in age-independent mortality explains a difference of 3 years out of the total of 9.69 years (or thirty-one percent). In relative terms, however, the reduction in age-independent mortality is the factor that has contributed the most to the increase in life expectancy for individuals in the 1st quintile (thirty-seven percent).

Third, the increase in the effective wage rate (or productivity growth) has also benefited

individuals in the highest quintile (2.7 years) by more than individuals in the lowest quintile (1.4 years).[14] Thus, the increase in wage rates accounts for a total difference of $1.3(= 2.7 - 1.4)$ years out of the total of 4.5 years (or twenty-nine percent) between individuals in the 1st and 5th quintile. For the uncontrolled case, the increasing wage rates explain 2.9 years out of the total of 9.69 (or thirty percent). Intuitively, a higher wage rate increases lifetime income, yielding a higher value of human capital and value of life, which in turn triggers additional health investments. Given that the share of health spending increases in income, higher paid individuals spend proportionally more on health than poorer individuals, widening the gap in life expectancy. Again, the spending differences are leveraged through medical progress.

Fourth, medical progress through the cardiovascular revolution explains thirty-three percent of the total number of additional years of life for individuals in the highest quintile (3.0 years) and thirty-six percent for individuals in the lowest quintile (1.7 years). See the green areas in Figure 8. Thus, the medical progress that started in the 1970s accounts for a gap in life expectancy at age 40 of $1.3(= 3.0 - 1.7)$ years between individuals in the 1st and 5th quintile groups. Thus, medical progress has also contributed another twenty-nine percent to the increasing gap in life expectancy across income groups. In the uncontrolled case, medical progress accounts for an increase of 3.1 years out of the 9.69. In addition, following Skinner and Staiger (2015) and considering that the access to the cardiovascular revolution differs across education groups (see yellow areas in Figure 8), our model estimates that the impact of medical progress on the life expectancy gap may account for an additional $0.7(= 0.5 - (-0.2))$ years, even in the uncontrolled case. Altogether, medical progress then explains a difference of 2.0 years out of the total of 4.5 years (or forty-four percent) of life expectancy growth between the 1st and 5th quintiles for the 1960 birth cohort and therefore it is the factor that has contributed the most to the increasing gap in life expectancy.

We conclude with the following observation. While selection explains about half of the widening in the life expectancy gap, it is in itself endogenous to the changes in the exogenous environment: cardiovascular medical progress, productivity growth, change in non-age related mortality and, to lesser degree, the educational gradient in the access to state-of-the-art medicine. In analogy to Figure 7 for the baseline scenario, we thus consider in Appendix H the frequency at which a set of unobservable characteristics from quintile u for the 1900 birth cohort is represented in quintile v for the 1960 birth cohort for each of the counterfactual scenarios (see Figures 14–17). While the frequencies are similar to those in the baseline (Figure 7) if the educational gradient in access to health care (Figure 15) or the change in non-age related mortality (Figure 17) are shut down, the frequencies remain strongly clustered on the diagonal if medical progress (Figure 14) or productivity growth (Figure 16) are shut down. This is a strong indication that, indeed, these two trends drive selection in a complementary way to the extent that if either one of them is shut down relatively little selection takes place.

Intuitively, selection into income groups is driven on the basis of selection into education groups as well as by (non-marginal) changes in behavioural patterns (such as e.g. the concomitant expansion of labor supply, savings and health care spending). The question then is what external changes, and for which types, trigger the behavioral changes that are underlying the selection into higher income quintiles. Recalling that the access to more effective medicine is tied to health investments, the absence of medical progress implies a stationary (low) return to health investments and, thus, constant health investments (at a low level)

[14] Recall that the increase in the wage rate per unit of human capital is assumed to be the same across both education groups. Despite this assumption, the model generates, in line with empirical findings, significant differences in the wage rate per hour worked across educational groups due to the positive impact of health on labor productivity and the change in the unobservable characteristics of each educational group.

and thus a stagnating life expectancy. There is little incentive then to engage in *additional* educational investments nor to supply *additional* labor in order to translate higher earnings into health investments and, thus, a longer life. Likewise, in the absence of productivity growth there is not enough scope to undertake the *additional* health investments warranted for sizeable gains in longevity beyond those afforded by medical progress to begin with. Thus, the different types of individuals tend to remain put with their given life-cycle patterns, implying only limited compositional change. The latter is triggered only by the joint emergence of medical progress and productivity growth. Selection then occurs, as it is (only) the most healthy types, standing to survive to high ages at which further advancements in longevity become feasible, who adopt behavioral changes that take them into higher income quintiles. In contrast, such behavioral change bears only limited return to the least healthy types with low life expectancy to begin with who do not effectively alter their behaviors to an extent that would advance them to higher income quintiles. Indeed, such a stifling of behavioral change is evidenced in the context of Huntington's disease, where those who are genetically predisposed show a much weaker propensity to invest in health and education (Oster et al., 2013).

6 Conclusion

We have devised a novel life-cycle model, based on demographic principles, that endogenously determines the most likely age at death. Individuals decide about their educational attainment, consumption path, labor supply, and health investments, conditional on a set of unobservable characteristics that control for heterogeneity in health, labor income, and education. The model has been calibrated using the Bayesian melding to replicate the evolution of the educational attainment, the distribution of income, and the death rates for US males born in 1900, 1920, 1940, and 1960.

In this paper, we show that our life-cycle model can accurately replicate the widening disparity in life expectancy across cohorts by socioeconomic status. Through counterfactual analyses, we find that medical progress, productivity growth, and the reduction in age-independent mortality have all positively contributed to the increase in life expectancy. When controlling for the initial characteristics of individuals, the model suggests that the relative contributions of medical progress, productivity growth, and the reduction in age-independent mortality are quite similar across income groups. However, medical progress has a slightly larger impact on the increasing gap in life expectancy at age forty across income groups compared to productivity growth and the reduction in age-independent mortality. We also find a strong role for selection. About half of the observed increase in the life expectancy gap between income groups over time can be attributed to selection, where lower income groups are becoming increasingly negatively selected in terms of health. Notably, however, the selection process itself is driven by the co-evolution of productivity growth and medical progress.

Our results suggest that in order to model the widening gap in life expectancy across socioeconomic status, it is necessary to develop models that account for the negative selection process within lower socioeconomic groups. The strong role of the selection process across cohorts also suggests that policies, such as universal health insurance, targeted provisioning of (state-of-the-art) health care, or educational campaigns, which are aimed at curbing the socio-economic gradient to the gains in longevity may need to be readjusted over time so as to keep track of the compositional changes, especially in regard to the underlying health traits, within observable social groups.

References

Aldy, J. E. and W. K. Viscusi (2008). Adjusting the Value of a Statistical Life for Age and Cohort Effects. *The Review of Economics and Statistics 90*(3), 573–581.

Bell, F. C. and M. L. Miller (2005). *Life tables for the United States social security area, 1900-2100*. Number 120. Social Security Administration, Office of the Chief Actuary.

Bergeron, A., R. Chetty, D. Cutler, B. Scuderi, M. Stepner, and N. Turner (2022). Replication Data for: The Association Between Income and Life Expectancy in the United States, 2001-2014.

Bloom, D. E., D. Canning, R. Kotschy, K. Prettner, and J. Schünemann (2024). Health and economic growth: Reconciling the micro and macro evidence. *World Development 178*, 106575.

Boucekkine, R., D. de la Croix, and O. Licandro (2002). Vintage human capital, demographic trends, and endogenous growth. *Journal of Economic Theory 104*(2), 340–375.

Canudas-Romo, V. (2008). The modal age at death and the shifting mortality hypothesis. *Demographic Research 19*, 1179–1204.

Cervellati, M. and U. Sunde (2013). Life Expectancy, Schooling, and Lifetime Labor Supply: Theory and Evidence Revisited. *Econometrica 81*(5), 2055–2086.

Chetty, R., M. Stepner, S. Abraham, S. Lin, B. Scuderi, N. Turner, A. Bergeron, and D. Cutler (2016). The Association Between Income and Life Expectancy in the United States, 2001–2014. *JAMA 315*(16), 1750–1766.

Costa, D. L. and M. E. Kahn (2004). Changes in the Value of Life, 1940-1980. *Journal of Risk and Uncertainty 29*(2), 159–180.

Cunha, F., J. Heckman, and S. Navarro (2005). Separating uncertainty from heterogeneity in life cycle earnings. *Oxford Economic Papers 57*(2), 191–261.

Cutler, D., A. Deaton, and A. Lleras-Muney (2006). The Determinants of Mortality. *The Journal of Economic Perspectives 20*(3), 97–120. Publisher: American Economic Association.

Dahl, G. B., C. T. Kreiner, T. H. Nielsen, and B. L. Serena (2024). Understanding the Rise in Life Expectancy Inequality. *The Review of Economics and Statistics 106*(2), 566–575.

Dalgaard, C.-J. and H. Strulik (2014). Optimal Aging and Death: Understanding the Preston Curve. *Journal of the European Economic Association 12*(3), 672–701.

Fonseca, R., P.-C. Michaud, T. Galama, and A. Kapteyn (2020). Accounting for the Rise of Health Spending and Longevity. *Journal of the European Economic Association 19*(1), 536–579.

Ford, E. S., U. A. Ajani, J. B. Croft, J. A. Critchley, D. R. Labarthe, T. E. Kottke, W. H. Giles, and S. Capewell (2007). Explaining the decrease in u.s. deaths from coronary disease, 1980–2000. *New England Journal of Medicine 356*(23), 2388–2398.

Frankovic, I. and M. Kuhn (2019). Access to health care, medical progress and the emergence of the longevity gap: A general equilibrium analysis. *The Journal of the Economics of Ageing 14*, 100188.

Frankovic, I., M. Kuhn, and S. Wrzaczek (2020). Medical innovation and its diffusion: Implications for economic performance and welfare. *Journal of Macroeconomics 66*, 103262.

Freiberger, M., M. Kuhn, A. Fürnkranz-Prskawetz, M. Sanchez-Romero, and S. Wrzaczek (2024). Optimization in age-structured dynamic economic models. *IIASA Working Paper. Laxenburg, Austria: WP-24-004*.

Gordon, R. (2017). *The rise and fall of American growth: The US standard of living since the civil war*. Princeton University Press.

Goujon, A., S. K.c, M. Speringer, B. Barakat, M. Potancoková, J. Eder, E. Striessnig, R. Bauer, and W. Lutz (2016). A harmonized dataset on global educational attainment between 1970 and 2060 – an analytical window into recent trends and future prospects in human capital development. *Journal of Demographic Economics 82*(3), 315–363.

Grossman, M. (1972). On the Concept of Health Capital and the Demand for Health. *Journal of Political Economy 80*(2), 223–255. Publisher: University of Chicago Press.

Hall, R. E. and C. I. Jones (2007). The Value of Life and the Rise in Health Spending*. *The Quarterly Journal of Economics 122*(1), 39–72.

Hansen, C. W. and H. Strulik (2017). Life expectancy and education: evidence from the cardiovascular revolution. *Journal of Economic Growth 22*, 421–450.

Horiuchi, S., N. Ouellette, S. L. K. Cheung, and J.-M. Robine (2013). Modal age at death: lifespan indicator in the era of longevity extension. *Vienna Yearbook of Population Research 11*, 37–69.

Huggett, M., G. Ventura, and A. Yaron (2011). Sources of Lifetime Inequality. *American Economic Review 101*(7), 2923–2954.

Human Mortality Database (2024). . Max Planck Institute for Demographic Research (Germany), University of California, Berkeley (USA), and French Institute for Demographic Studies (France). Available at www.mortality.org. Data downloaded on 3-20-2024.

Keane, M. P. (2022). Recent research on labor supply: Implications for tax and transfer policy. *Labour Economics 77*(C). Publisher: Elsevier.

Kotschy, R. (2021). Health dynamics shape life-cycle incomes. *Journal of Health Economics 75*, 102398.

Kuhn, M., S. Wrzaczek, A. Prskawetz, and G. Feichtinger (2015). Optimal choice of health and retirement in a life-cycle model. *Journal of Economic Theory 158*, 186–212.

Lee, R., A. Mason, and T. Miller (2000). Life cycle saving and the demographic transition: The case of taiwan. *Population and Development Review 26*, 194–219.

Lee, R. and M. Sanchez-Romero (2019). Overview of Heterogeneity in Longevity and Pension Schemes. In *Progress and Challenges of Nonfinancial Defined Contribution Pension Schemes: Volume 1. Addressing Marginalization, Polarization, and the Labor Market*, pp. 259–279. The World Bank.

Lee, R. D. and L. R. Carter (1992). Modeling and Forecasting U. S. Mortality. *Journal of the American Statistical Association 87*(419), 659–671.

Lexis, W. H. R. A. (1879). *Sur la durée normale de la vie humaine et sur la théorie de la stabilité des rapports statistiques*. Vve. F. Henry.

Link, B. G. and J. Phelan (1995). Social Conditions As Fundamental Causes of Disease. *Journal of Health and Social Behavior*, 80–94.

Missov, T., A. Lenart, L. Nemeth, V. Canudas-Romo, and J. W. Vaupel (2015). The Gompertz force of mortality in terms of the modal age at death. *Demographic Research 32*, 1031–1048.

Murtin, F., J. P. Mackenbach, D. Jasilionis, and M. M. d'Ercole (2022, March). Educational inequalities in longevity in 18 OECD countries. *Journal of Demographic Economics 88*(1), 1–29.

NASEM and others (2015). *The growing gap in life expectancy by income: Implications for Federal programs and policy responses*. Washington, D.C.: National Academies Press.

Nishiyama, S. and K. Smetters (2014). Chapter 3 - Analyzing Fiscal Policies in a Heterogeneous-Agent Overlapping-Generations Economy. In K. Schmedders and K. L. Judd (Eds.), *Handbook of Computational Economics*, Volume 3 of *Handbook of Computational Economics Vol. 3*, pp. 117–160. Elsevier.

OECD (2017). *Preventing Ageing Unequally*. Paris: Organisation for Economic Co-operation and Development.

Oreopoulos, P. (2007). Do dropouts drop out too soon? Wealth, health and happiness from compulsory schooling. *Journal of Public Economics 91*(11), 2213–2229.

Oster, E., I. Shoulson, and E. R. Dorsey (2013). Limited life expectancy, human capital and health investments. *The American Economic Review 103*(5), 1977–2002.

Poole, D. and A. E. Raftery (2000). Inference for Deterministic Simulation Models: The Bayesian Melding Approach. *Journal of the American Statistical Association 95*(452), 1244–1255.

Restuccia, D. and G. Vandenbroucke (2013). A Century of Human Capital and Hours. *Economic Inquiry 51*(3), 1849–1866.

Rockwood, K. and A. Mitnitski (2007). Frailty in relation to the accumulation of deficits. *The Journals of Gerontology. Series A, Biological Sciences and Medical Sciences 62*(7), 722–727.

Rosen, S. (1988). The Value of Changes in Life Expectancy. *Journal of Risk and Uncertainty 1*(3), 285–304.

Sánchez-Romero, M., H. d'Albis, and A. Prskawetz (2016). Education, lifetime labor supply, and longevity improvements. *Journal of Economic Dynamics and Control 73*, 118–141.

Sánchez-Romero, M., R. D. Lee, and A. Prskawetz (2020). Redistributive effects of different pension systems when longevity varies by socioeconomic status. *The Journal of the Economics of Ageing 17*, 100259.

Sánchez-Romero, M., P. Schuster, and A. Prskawetz (2023). Redistributive effects of pension reforms: who are the winners and losers? *Journal of Pension Economics and Finance*, 1–27.

Skinner, J. and D. Staiger (2015). Technology Diffusion and Productivity Growth in Health Care. *The Review of Economics and Statistics 97*(5), 951–964.

Smith, J. P. (2007). The Impact of Socioeconomic Status on Health over the Life-Course. *The Journal of Human Resources 42*(4), 739–764.

Stephens Jr., M. and D. Toohey (2022). The Impact of Health on Labor Market Outcomes: Evidence from a Large-Scale Health Experiment. *American Economic Journal: Applied Economics 14*(3), 367–399.

Sánchez-Romero, M. and A. Prskawetz (2017, December). Redistributive effects of the US pension system among individuals with different life expectancy. *The Journal of the Economics of Ageing 10*, 51–74.

U.S. Census Bureau (2001). *Money Income in the United States, 2000.* U.S. Government Printing Office, Washington, DC.

van Kippersluis, H., O. O'Donnell, E. van Doorslaer, and T. Van Ourti (2010). Socioeconomic differences in health over the life cycle in an Egalitarian country. *Social Science & Medicine 70*(3), 428–438.

Vaupel, J. W., K. G. Manton, and E. Stallard (1979). The impact of heterogeneity in individual frailty on the dynamics of mortality. *Demography 16*(3), 439–454.

Waldron, H. (2007). Trends in mortality differentials and life expectancy for male social security-covered workers, by socioeconomic status. *Social Security Bulletin 67*(3), 1–28.

Weil, D. N. (2007). Accounting for the Effect Of Health on Economic Growth. *The Quarterly Journal of Economics 122*(3), 1265–1306.

A Life cycle model

The problem of the individual is to maximize (5) subject to (1)–(3), (6), (7) and the boundary conditions on capital $k(0) = k(T) = 0$. To solve the problem we use the following current-value Hamiltonian

$$\begin{aligned}\mathcal{H} =& S(U(c,\ell) - \xi_e \mathbf{1}(t \leq E)) \\ &+ \lambda_k(rk + wH\ell\mathbf{1}(t > E) - c - m) \\ &+ \lambda_H\big(\xi_h H^{\gamma_h}\mathbf{1}(t \leq E) + f(t,E)H\mathbf{1}(t > E) - \phi\mu(M)H\big) \\ &- \lambda_S\mu(M)S \\ &+ \lambda_M A m^{\gamma_m},\end{aligned} \tag{20}$$

and the inequality conditions $\nu_1(1-\ell)$ and $\nu_2\ell$. The term $\mathbf{1}(\cdot)$ is an indicator function that takes the value of one when the inequality is satisfied and zero otherwise, and $(\lambda_k, \lambda_H, \lambda_S, \lambda_M)$ are the set of shadow prices associated with the state variables: capital (k), human capital (H), survival (S), and modal age at death (M), respectively.

Solution Given number of years of schooling E, to achieve a maximum the individual problem must fulfill the following necessary conditions for all $t \in [0, T]$:

- First-order conditions (FOCs):

$$\begin{aligned} c: &\qquad \lambda_k = SU_c \\ \ell: &\qquad wH\lambda_k = -SU_\ell + \nu_1 - \nu_2 \text{ for } t > E \\ m: &\qquad \lambda_k = \lambda_M A\gamma_m m^{\gamma_m - 1}\end{aligned}$$

  where ν_1 and ν_2 are the Lagrange multipliers associated with the Kuhn-Tucker conditions.

- Envelope conditions (ECs):

$$\begin{aligned}\dot{\lambda}_k &= \lambda_k(\rho - r) \\ \dot{\lambda}_H &= \lambda_H\big(\rho - \xi_h\gamma_h H^{\gamma_h - 1}\mathbf{1}(t \leq E) - f(t,E)\mathbf{1}(t > E) + \phi\mu(M)\big) - \lambda_k w\ell\mathbf{1}(t > E) \\ \dot{\lambda}_S &= \lambda_S(\rho + \mu(M)) - \big(U(c,\ell) - \xi_e\mathbf{1}(t \leq E)\big) \\ \dot{\lambda}_M &= \lambda_M\rho + \mu'(M)(\lambda_H\phi H + \lambda_S S)\end{aligned}$$

- Transversality conditions (TCs)

$$\lambda_k(T) > 0, \qquad \lambda_H(T) = \lambda_S(T) = \lambda_M(T) = 0$$

- Optimal maximum age condition

$$\mathcal{H}(\mathbf{x}(T^*), \mathbf{X}(T^*), \boldsymbol{\lambda}(T^*), T^*) = 0,$$

  where $\mathbf{x}(T)$ is the vector of controls at time T $(c(T), \ell(T), m(T))$, $\mathbf{X}(T)$ is the vector of states at time T $(k(T), H(T), S(T), M(T))$, and $\boldsymbol{\lambda}(T)$ is the vector of adjoints at time T $(\lambda_k(T), \lambda_H(T), \lambda_S(T), \lambda_M(T))$. This condition implies that the optimal maximum longevity T is reached when the value of life is equal to the instantaneous consumption; i.e. $U/U_c = c$. For computational issues, we define a $T^{\star\star}$ such that $S(T^{\star\star}) \approx 10^{-3}$ and impose the restriction that $T = \min\{T^*, T^{\star\star}\}$.

- Optimal educational attainment: Given the optimal path of consumption, health investments, labor supply, and the maximum age condition for each possible E, the individual chooses the number of years of education that maximizes (5).

B Frailty model

In this section we show that our mortality hazard rate contains features of the health-deficit model (Dalgaard and Strulik, 2014), the Lee-Carter model Lee and Carter (1992), and the frailty model (Vaupel et al., 1979). To do so, we use the definition of the mortality hazard rate in terms of the modal age at death

$$\mu(t, M(t)) = c_\mu + be^{b(t-M(t))}.$$

Substituting the modal age at death at time t by the integral from 0 to t of (3) gives

$$\mu(t, M(t)) = c_\mu + be^{bt-b\left(M_0+\int_0^t A(s)m(s)^{\gamma_m}ds\right)}.$$

where $M_0 \sim \mathcal{N}(\mu_M, \sigma_M^2)$ is the initial modal age at death, which is distributed according to a normal distribution with mean μ_M and standard deviation σ_M, and the integral term is the total increase in the modal age at death from age 0 until age t, which we will denote from now on by $\Delta M(t) = \int_0^t A(s)m(s)^{\gamma_m}ds$. Multiplying the terms inside the parenthesis by the natural rate of ageing, we have

$$\mu(t, M(t)) = c_\mu + be^{bt-bM_0-b\Delta M(t)}. \tag{21}$$

Ageing process. A realistic feature of the health-deficit model (Dalgaard and Strulik, 2014) is that individuals accumulate health deficits as they age. The higher are the number of health deficits, the faster they accumulate (i.e. the faster is the ageing process), and the greater is the probability of dying. Individuals can reduce the speed of aging by investing in health. This feature is shared in our framework. Taking the logarithm of the difference between the mortality rate and the age-independent mortality (i.e. the Makeham component) and differentiating with respect to t gives the speed of ageing or the senescence rate

$$\frac{\partial}{\partial t}\log(\mu(t, M(t)) - c_\mu) = b(1 - A(t)m(t)^{\gamma_m}). \tag{22}$$

The above equation shows that similar to the health-deficit model (Dalgaard and Strulik, 2014), individuals can reduce the senescence rate from it's natural level, b, by investing in health. In particular, given an initial modal age at death M_0 our model implies that individuals who invest more (resp. less) in health will have a lower (resp. higher) senescence rate and hence a higher probability of living longer.

Lee-Carter model. Similar to the Lee and Carter (1992) model, our senescence rate will not change monotonously over the life cycle due to the fact that health investments vary non-monotonously over the life span. Rearranging Eq. (21) and taking the log, we obtain

$$\log\left(\mu(t, M(t)) - c_\mu\right) = \underbrace{\log be^{b(t-\mu_{M_0})}}_{\mathbf{a}_t} + \underbrace{(-b)\Delta M(t)}_{\mathbf{b}_x\mathbf{k}_t} + \underbrace{(-b)(M_0 - \mu_M)}_{\epsilon},$$

where the first term on the right hand side corresponds to the general shape of the mortality schedule $\mathbf{a}_t$, the second term corresponds to the rate of decline in mortality over time $\mathbf{b}_x\mathbf{k}_t$, and the last term is the residual term $\epsilon \sim \mathcal{N}(0, b^2\sigma_M^2)$ in the Lee-Carter model.

Frailty model. By rearranging the terms in (21) we obtain the standard frailty model (Vaupel et al., 1979) augmented with gains in senescence

$$\begin{aligned}\mu(t, M(t)) &= c_\mu + e^{\log b - bM_0 + bt - b\Delta M(t)} \\ &= c_\mu + Zae^{b(1-t^{-1}\Delta M(t))t},\end{aligned} \tag{23}$$

where

$$Z = \exp\left\{-b(M_0 - \mu_M) - \frac{b^2\sigma_M^2}{2}\right\}$$
$$a = \exp\left\{\log b - b\mu_M + \frac{b^2\sigma_M^2}{2}\right\}$$

There are several key findings from (23). The first thing to notice is that the mortality hazard rate exactly coincides with the frailty model when there are no health investments (i.e. $\Delta M(t) = 0$). Second, given that $\mathbf{E}[Z]$ is equal to zero by definition, we obtain that in two populations with similar μ_M, the population with the highest σ_M^2 will have on average a higher mortality than the population with the lowest σ_M^2 (Vaupel et al., 1979).

C Age-Specific Mortality Rates by Educational Attainment

We compute period life tables by education based on the *Mortality Multiple Cause Files* provided by the Centers for Disease Control and Prevention (from now on *CDC data*).[15] These data contain information about the resident status, age, education level, and the cause of death for defunct people on a yearly basis. The *CDC data* for years earlier than 1989 do not provide information about education, and therefore we restrict the data to the 1989-2019 period. We only consider US-residents for which age is known, reported in years, and smaller or equal to 100. We recode the causes of death following the shortlist of causes of death provided by the *Human Cause-of-Death Database (HCD)*.[16] The shortlist of causes of death is the same for all countries contained in the HCD database and contains 16 different causes of death. The causes of death in the CDC data before 1999 are coded using ICD-9 codes, which for comparability with successive years we convert into ICD-10 codes using the conversion tables provided by the Canadian Institute for Health Information (CIHI).[17] Some ICD-9 codes cannot be converted. As these codes are unrelated to heart diseases, we group them and convert the underlying cases to *Other causes*. It is important that heart diseases are converted correctly since they are used to build the counterfactual mortality rates under the presumption that the cardiovascular revolution had not occurred.

We merge the IPUMS USA population data with the CDC data to estimate the mortality rates by education for male US-residents using the year of observation, age, and highest educational attainment. We are able to compute mortality rates by educational attainment for 1990, 2000, and yearly from 2000 to 2019 because the IPUMS USA population data are available only on a decennial basis for years earlier than 2000. The educational attainment, for both the CDC data and the IPUMS USA data, is recoded such that we obtain two distinct groups, college and less than college. We assign individuals with more than 12 years

[15] https://www.cdc.gov/nchs/data_access/vitalstatsonline.htm

[16] https://www.mortality.org/Data/HCD

[17] https://secure.cihi.ca/free_products/conversion-tables-ICD10CA-ICD9-ICD9CM-CCI-CCP-en.xlsx

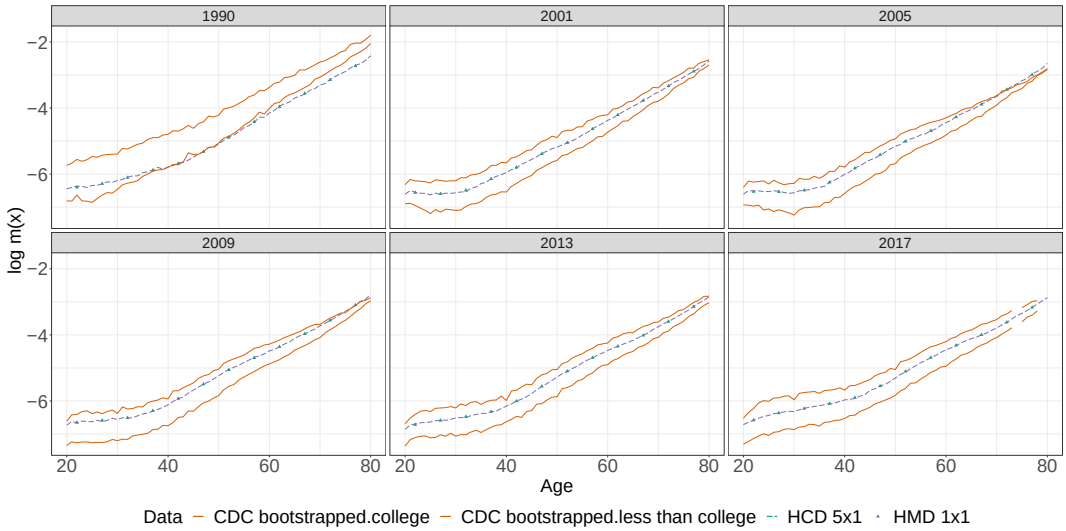

Figure 9: Mortality Rates: mortality rates by educational attainment as estimated from CDC data as compared to the mortality rates for males obtained from the Human Mortality Database (HMD) and the Human Cause of Death Database (HCD).

of completed education to the *college* group, with 12 or less than 12 years of completed education to the *less-than-college* group, whereas individuals with no formal education are not considered. Since the CDC data contain observations with unknown education, we estimate bootstrapped mortality rates by cause of death for US-resident males aged between 20 and 95 years. First, we exclude observations with unknown educational attainment from the CDC data. Then we compute the share of observations excluded by age and year of observation, exclude the same share of observations by age and year of observation from the IPUMS USA population data - the educational attainment of the excluded individuals is random - and compute the mortality rates by year, age, education and cause of death using the resulting population by year, age and education. We repeat this process 1,000 times and average over the obtained mortality rates to obtain robust bootstrapped mortality rates by year, age education and cause of death. If there is no unknown educational attainment for a combination of age, year and cause of death, we do not need to estimate bootstrapped mortality rates. The mortality rates by education and year are not smooth for higher ages, most of the time mortality rates start becoming erratic from age 80 to 85 onwards. To smooth the mortality rates we apply a Kannisto model for ages above 80. Finally, we estimate the life table by education for males resident in the United States between ages 20 and 95. In Figure 9 we compare the estimated log-mortality rates by education to the log- mortality rates from the Human Mortality database (HMD) and the Human Cause-of-Death database (HCD).[18][19] Our estimates appear to be consistent with the HMD and HCD mortality rates since both lie between the mortality rates for higher (college) and lower (less-than-college) educated people.

[18] https://www.mortality.org/
[19] https://www.mortality.org/Data/HCD

D Wage rate estimation

To estimate the components (β_1, β_2, ϕ) of the wage equation we collected individual data from IPUMS USA on labor income and on the average number of hours worked by age, year, education, industry, occupation and race. We calculated the years of experience as the difference between the age of each individual and the age at completing school, and we grouped the years of experience into five-year intervals. Before estimating the returns to experience (β_1, β_2), we regressed the logarithm of the wage rate per hour worked using the fixed effects model $\log w_{etios} = \rho_E E + \gamma_e + \gamma_t + \gamma_i + \gamma_o + \gamma_s + \epsilon_{etios}$, where ρ_E is the return to education, E denotes the additional years of education starting from age 14, γ_e is the experience fixed effect, γ_t is the year fixed effect, γ_i is the industry fixed effect, γ_o is the occupation fixed effect, and γ_s is the state fixed effect.

Table 3 presents results for three alternative models. In model (1) both education groups (college and non-college) are included into the regression, whereas models (2) and (3) provide regressions for the two education groups in separate. From the regression results on the years of experience from model (1) we approximated the working ability profile using a quadratic function of the years of experience $\hat{\gamma}_e = \text{Ct} + \beta_1 \text{Exp} + \beta_2 \text{Exp}^2 + u_e$, where Ct is a constant term, Exp is the years of experience, and u_e is the error term.

Table 3: Estimated return on experience by education

	Dependent variable: log(wage per hour)		
	Aggregated education	college	less than college
	(1)	(2)	(3)
5 to 9 years of experience	0.223***	0.211***	0.171***
	(0.010)	(0.014)	(0.017)
10 to 14 years of experience	0.381***	0.404***	0.319***
	(0.010)	(0.013)	(0.016)
15 to 19 years of experience	0.494***	0.510***	0.421***
	(0.010)	(0.013)	(0.016)
20 to 24 years of experience	0.564***	0.552***	0.471***
	(0.009)	(0.012)	(0.015)
25 to 29 years of experience	0.585***	0.560***	0.506***
	(0.009)	(0.012)	(0.015)
30 to 34 years of experience	0.593***	0.547***	0.511***
	(0.010)	(0.013)	(0.016)
35 to 39 years of experience	0.630***		0.514***
	(0.013)		(0.017)
returns to education: college	0.047***		
	(0.001)		
returns to education: less than college	0.035***		
	(0.001)		
returns to education		0.060***	0.024***
		(0.001)	(0.001)
Constant	2.167***	2.058***	2.400***
	(0.043)	(0.068)	(0.065)
Total Weighted Observations	12,552,970	6,532,227	6,020,743
Observations	101,258	58,800	42,458
Adjusted R^2	0.316	0.238	0.176
Residual Std. Error	0.602 (df = 101172)	6.882 (df = 58716)	6.514 (df = 42373)
Note:			*p<0.1; **p<0.05; ***p<0.01

E Bayesian melding

Let $F(\cdot)$ denote our lifecycle model. The model is used to replicate the educational, mortality, and income distribution of the cohorts born in 1900, 1920, 1940, and 1960 in the US. Each cohort is assumed to be represented by a set of $J = 1\,000$ heterogeneous agents, whose permanent and unobservable characteristics are randomly assigned at birth and are identical across cohorts. Let the set of permanent and unobservable characteristics of the j-th agent be $(M_{0j}, \xi_{h,j}, \xi_{e,j})$, where M_{0j} is the initial modal age at death, ξ_{hj} is the learning ability level, and ξ_{ej} is the effort of schooling. The initial modal age at death M_0 is assumed to be Normal-distributed $\mathcal{N}(\mu_M, \sigma_M^2)$. The pair of unobservable characteristics (ξ_h, ξ_e) are assumed to be drawn from a bivariate Clayton copula formed by two Gamma distributions

$$(\xi_h, \xi_e) \sim C\left(\Gamma_1\left(\frac{\mu_{\xi_h}^2}{\sigma_{\xi_h}^2}, \frac{\sigma_{\xi_h}^2}{\mu_{\xi_h}}\right), \Gamma_2\left(\frac{\mu_{\xi_e}^2}{\sigma_{\xi_e}^2}, \frac{\sigma_{\xi_e}^2}{\mu_{\xi_e}}\right)\right) \tag{24}$$

Let $\mathcal{D}$ denote the combination of the normal distribution and the copula; i.e. $\mathcal{D} = \mathcal{N} \times C(\Gamma_1, \Gamma_2)$. Our calibration problem involves seven parameters or inputs,

$$\theta = (\mu_M, \sigma_M, \mu_{\xi_h}, \mu_{\xi_e}, \sigma_{\xi_h}, \sigma_{\xi_e}, \rho_\xi) \in \Theta \subseteq \mathbb{R}^7$$

taken from the feasible parameter set

$$\Theta = (\underline{\mu_M}, \overline{\mu_M}) \times (\underline{\gamma_m}, \overline{\gamma_m}) \times (\underline{\mu_{\xi_h}}, \overline{\mu_{\xi_h}}) \times (\underline{\sigma_{\xi_h}}, \overline{\sigma_{\xi_h}}) \times (\underline{\mu_{\xi_e}}, \overline{\mu_{\xi_e}}) \times (\underline{\sigma_{\xi_e}}, \overline{\sigma_{\xi_e}}) \times (\underline{\rho_\xi}, \overline{\rho_\xi}),$$

where the symbols $\underline{x}$ and $\overline{x}$ denote the minimum and maximum value of parameter x, respectively. The pair (μ_M, σ_M) is the mean and the standard deviation of the initial modal age at death, μ_{ξ_h} is the average learning ability, μ_{ξ_h} is the average effort of schooling, σ_{ξ_h} is the standard deviation of the learning ability, σ_{ξ_e} is the standard deviation of the effort of schooling, and ρ_ξ is the absolute value of the correlation between learning ability and effort of schooling.

Let the prior distribution on inputs $p(\Theta)$ be the product of uninformative priors $p(\Theta) = \mathcal{U}(\Theta)$. Let $\phi \in \Phi$ be the set of outputs generated from the model F given the inputs θ; i.e. $F(\theta) = \phi$. Let us denote by ϕ^C the set of outputs used for the calibration and by ϕ^N the set of outputs not used for the calibration, i.e. $\phi = (\phi^C, \phi^N)$. The outputs ϕ^C are a sequence of economic and demographic data for the 1900, 1920, 1940, and 1960 birth cohorts, which we will fit to actual data. In particular, we generate: i) the fraction of individuals within each birth cohort with non-college education $\phi^{1C}(\theta)$; ii) the average cohort-life expectancy at age 14 for each birth cohort $\phi^{2C}(\theta)$; iii) the wage rate distribution of workers aged 40–44, who were born in year 1960, with non-college education $\phi^{3C}(\theta)$ and with college education $\phi^{4C}(\theta)$, respectively; iv) education- and age-specific mortality rates for the 1940 and 1960 birth cohorts; and v) age-specific mortality rates for the 1900, 1920, 1940, and 1960 birth cohorts.[20] Let the prior distribution on outputs used for the calibration $q(\Phi^C)$ be

$$q(\Phi^C) = \prod_{j=1}^{4} q_j(\Phi^{jC}) \text{ with } q_j(\Phi^{jC}) = \begin{cases} 1 & \text{if } ||\phi^{jC}(\Theta) - \widehat{\phi}^{jC}|| < \Delta_j\sqrt{n}, \\ \epsilon & \text{otherwise,} \end{cases}$$

where $\widehat{\phi}^{jC}$ is the vector of observed data for sequence j and Δ_j is the maximum threshold allowed for the difference between the generated and the observed sequence of data j.

[20] To generate the data for each birth cohort, we draw a sample of N individuals with their unobservable characteristics for a given set of inputs $\theta \in \Theta$ using the distribution $\mathcal{D}$.

Let the likelihood of the model's output for calibration ϕ^C be given by

$$\mathcal{L}(\phi^C|\text{data}) \propto \exp\left\{-\frac{1}{2}\sum_{j=1}^{4}(\phi^{jC}(\theta) - \widehat{\phi}^{jC})^T \mathbf{W}_j^{-1}(\phi^{jC}(\theta) - \widehat{\phi}^{jC})\right\} \tag{25}$$

where $\mathbf{W}_j$ is the weighted matrix for the sequence of data j, which is assumed to be an identity matrix $\mathbf{I}$.

We implement the Bayesian melding with the IMIS algorithm, with the prior as importance sampling distribution. Specifically, we pursue the following steps:

- Initial stage:
  1. Draw $N_0 = 7\,000$ independent and identically distributed (i.i.d.) samples, $\{\theta_1, \ldots, \theta_{N_0}\}$, from the joint prior distribution on inputs $p(\Theta)$.
  2. For each θ_i sampled, run the model to obtain the set of outputs, i.e. $F(\theta_i) = \phi_i^C$.
  3. Calculate the likelihood of each model output ϕ_i^C
  $$\mathcal{L}(\phi_i^C|\text{data}) \text{ for } i = \{1, \ldots, N_0\}$$
  4. Construct the importance weights for each θ_i
  $$\omega(\theta_i) \propto \frac{q(\phi_i^C)\mathcal{L}(\phi_i^C|\text{data})}{\sum_{i=1}^{N} q(\phi_i^C)\mathcal{L}(\phi_i^C|\text{data})} \text{for } i = \{1, \ldots, N_0\}$$
- Importance Sampling Stage: For $k = 1, 2, \ldots$
  1. Choose the current maximum weight input as the center
  $$\theta^{(k)} = \arg\max_{\theta \in \{\theta_1, \ldots, \theta_{N_{k-1}}\}} \left(w(\theta_1), \ldots, w(\theta_{N_{k-1}})\right)$$
  .
  2. Estimate $\Sigma^{(k)}$ as the weighted covariance of the $B = 100$ inputs with the smallest Mahalanobis distances to $\theta^{(k)}$, where the distances are calculated w.r.t. the covariance of the prior distribution and the weights are $\left(w(\hat{\theta}_1) + \frac{1}{N_k}, \ldots, w(\hat{\theta}_B) + \frac{1}{N_k}\right)$. The Mahalanobis distance is:
  $$d(\theta, \theta^{(k)}) = \sqrt{(\theta - \theta^{(k)})' * Q * (\theta - \theta^{(k)})}$$
  where Q is the covariance matrix of the prior distribution on inputs
  3. Sample B new inputs $(\theta_{N_{k-1}+1}, \ldots, \theta_{N_{k-1}+B})$ from the multivariate Gaussian distribution
  $$H_k : \mathcal{N}(\theta^{(k)}, \Sigma^{(k)}) \tag{26}$$
  4. Calculate the likelihood of the new inputs and combine the new inputs with the previous ones. Form the importance weights:
  $$w(\theta_i) = c \cdot q_2(\phi_i^C)\mathcal{L}(\phi_i^C) \times \frac{p(\theta_i)}{q^{(k)}(\theta_i)} \text{ for } i = N_{k-1} + 1, \ldots, N_k. \tag{27}$$
  with $q^{(k)}(\theta_i) = \frac{N_0}{N_k} p(\theta_i) + \frac{B}{N_k}\sum_{s=1}^{k} H_s(\theta_i)$, where $H_s(\theta_i)$ is the probability of having input θ_i in the multivariate Gaussian distribution $\mathcal{N}(\theta^{(s)}, \Sigma^{(s)})$, c is a scaling factor that guarantees $\sum_i^{N_k} w(\theta_i) = 1$, and $N_k = N_0 + kB$.

- Resample stage: Once the expected fraction of unique points in the resample $\sum_{i=1}^{N_k}(1-(1-w(\theta_i))^J)$ is at least 0.632 out of 3 500 random draws, we resample $J = 200$ inputs with replacement from $\{\theta_1, \ldots, \theta_{N_k}\}$ with weights $\{\omega(\theta_1), \ldots, \omega(\theta_{N_k})\}$ to approximate the posterior distribution of the inputs and outputs.

The model and the Bayesian melding with the IMIS algorithm have been programmed in Julia. To find the initial co-state variables of the life cycle model, we have used the Mixed Complementary Problems solvers contained in the NLSolve package. The Bayesian melding has reached the stopping criteria after 55 iterations.

Marginal posterior distribution of inputs Figure 10 shows the marginal posterior distribution of the model inputs θ. Figure 10 suggests the existence of multiple combinations of $\theta \in \Theta$ that provide a likely fit to the data. Therefore, the Bayesian melding is a good option for calibrating the model in order to avoid invertibility problems (Poole and Raftery, 2000). Moreover, an important feature of the calibration strategy is that it is not necessary to run sensitivity analysis against these parameters. This is because the calibration already provides the results of combining different parameters values.

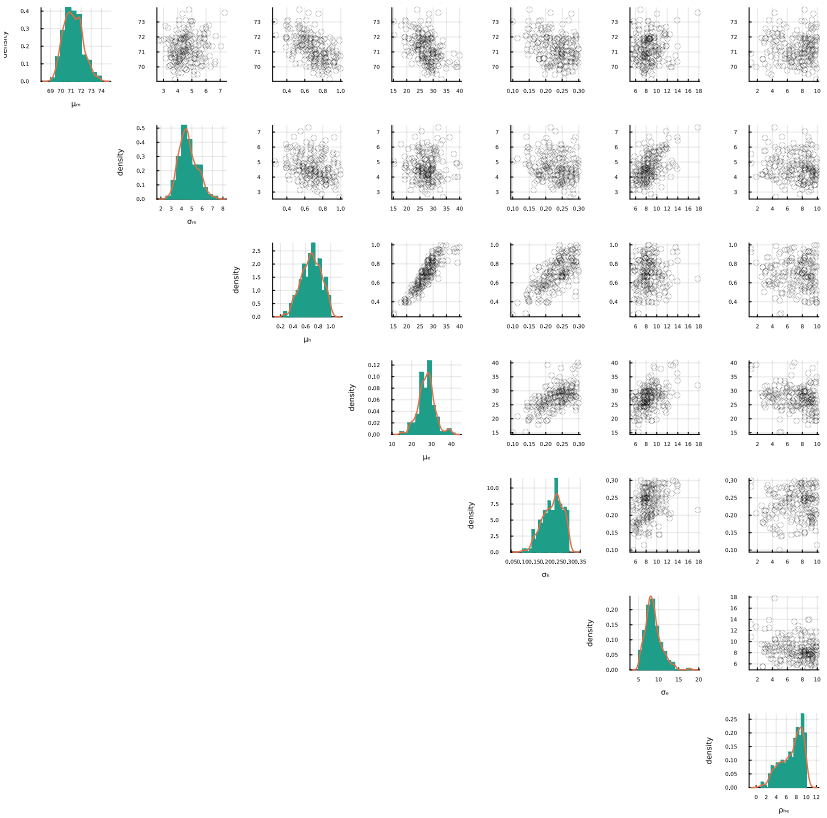

Figure 10: Marginal posterior distributions of inputs θ. The terms μ_M, γ_m, μ_{ξ_h}, σ_{ξ_h}, μ_{ξ_e}, σ_{ξ_e}, ρ_ξ stand for the average initial modal age at death, the standard deviation (std.) of the initial modal age at death, the mean learning ability, the std. of the learning ability, the mean effort of schooling, the std. of the effort of schooling, and the correlation between the learning ability and the effort of schooling, respectively.

F Contributions to the increase in life expectancy across cohorts at different ages

Cohort	Baseline	Education-specific time of benefiting from the CVR†	Effective wage increase	Medical technological progress	Reduction age-independent mortality
Age = 15					
1920	5.92	0.15 (2.5%)	2.52 (42.6%)	1.49 (25.2%)	1.75 (29.6%)
1940	7.67	0.16 (2.1%)	2.66 (34.7%)	2.43 (31.7%)	2.42 (31.6%)
1960	9.61	0.09 (1.0%)	2.97 (30.9%)	3.32 (34.5%)	3.24 (33.7%)
Age = 40					
1920	3.24	0.10 (3.1%)	1.30 (40.1%)	0.85 (26.2%)	0.99 (30.6%)
1940	5.01	0.11 (2.2%)	1.67 (33.3%)	1.62 (32.3%)	1.60 (31.9%)
1960	6.86	0.08 (1.2%)	2.08 (30.3%)	2.38 (34.7%)	2.32 (33.8%)
Age = 65					
1920	1.96	0.07 (3.6%)	0.69 (35.2%)	0.58 (29.6%)	0.63 (32.1%)
1940	3.48	0.10 (2.9%)	1.10 (31.6%)	1.16 (33.3%)	1.12 (32.2%)
1960	4.92	0.08 (1.6%)	1.48 (30.1%)	1.71 (34.8%)	1.65 (33.5%)

Table 4: Contributions of different factors to the overall increase in life expectancy at different ages from the 1900 birth cohort. Note: † CVR stands for cardiovascular revolution.

G Contribution of exogenous factors to the increase in life expectancy at age 40 from the 1900 to 1960 birth cohorts by wage quintile

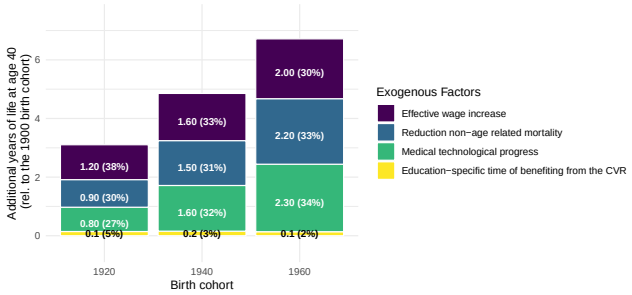

(a) Uncontrolled

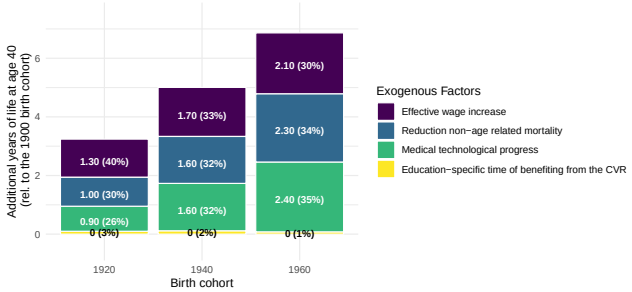

(b) Reference group: Wage quintiles for the 1960 birth cohort

Figure 11: Contribution of exogenous factors to the increase in life expectancy at age 40 from the 1900 to 1960 birth cohorts by wage quintile.

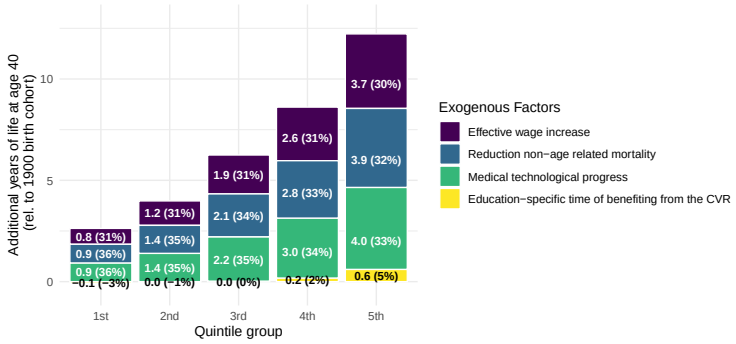

(a) Uncontrolled

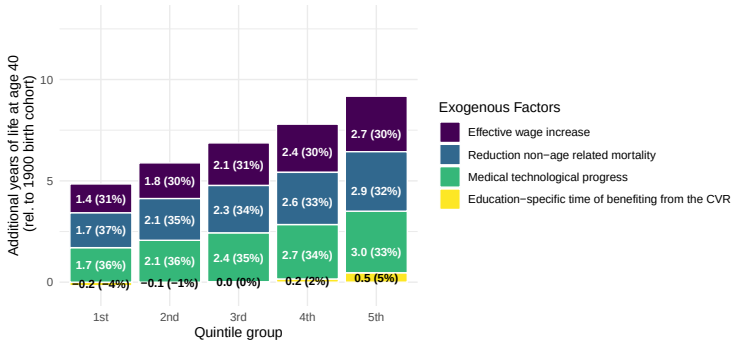

(b) Reference group: Wage quintiles for the 1960 birth cohort

Figure 12: Contribution of exogenous factors to the increase in life expectancy at age 40 from the 1900 to 1960 birth cohorts by wage quintile.

H Distribution of the initial characteristics across birth cohort and income groups

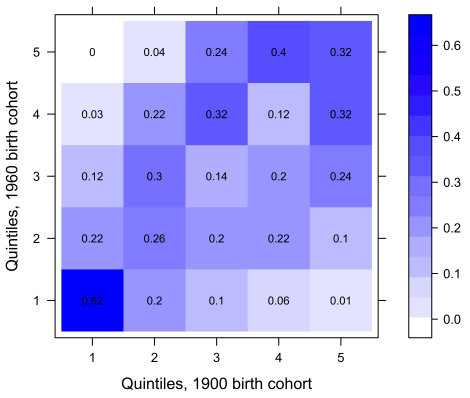

(a) Frequency

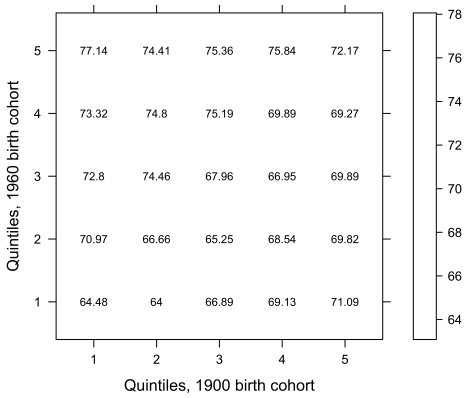

(b) Modal age at death (M_0)

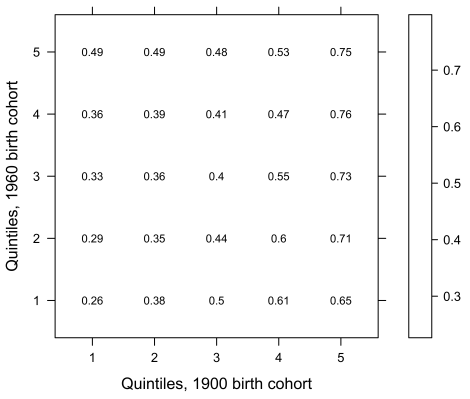

(c) Learning ability (ξ_h)

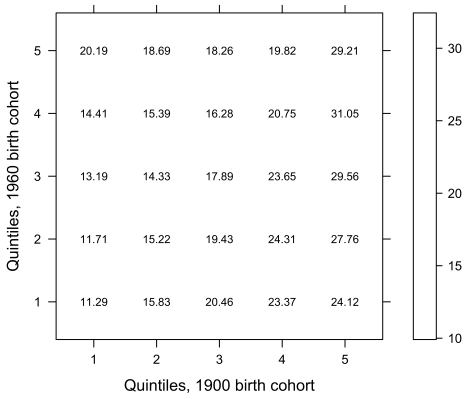

(d) Effort of schooling (ξ_e)

Figure 13: Distribution of the initial (unobservable) characteristics by wage quintile and birth cohort in the baseline simulation.

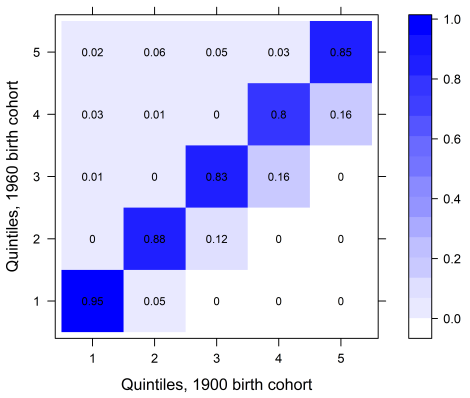

(a) Frequency

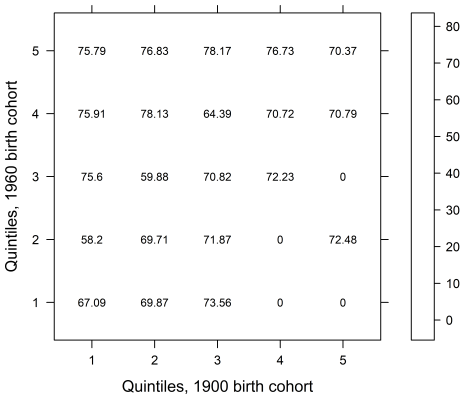

(b) Modal age at death (M_0)

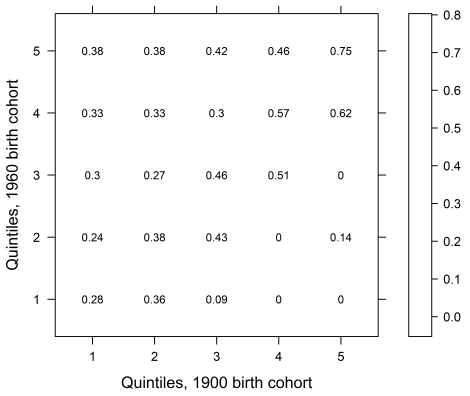

(c) Learning ability (ξ_h)

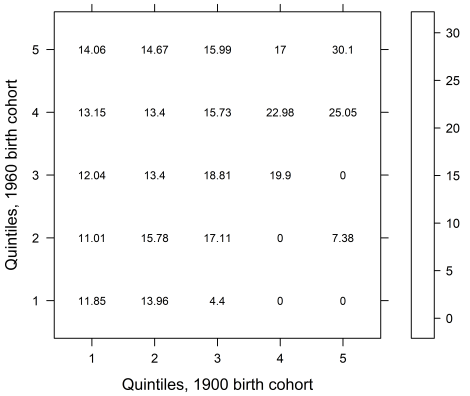

(d) Effort of schooling (ξ_e)

Figure 14: Distribution of the initial (unobservable) characteristics by wage quintile and birth cohort when medical technology is shut down.

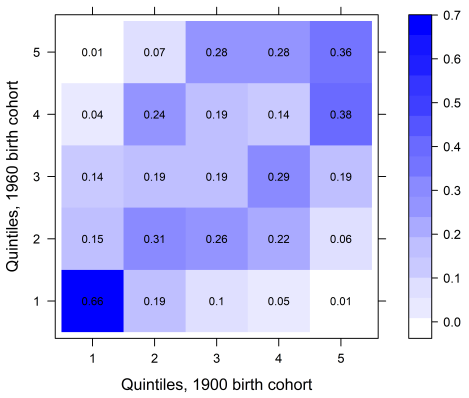

(a) Frequency

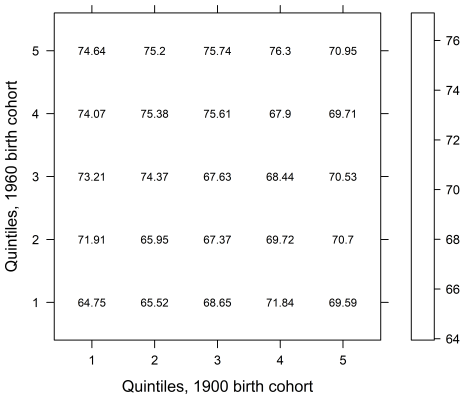

(b) Modal age at death (M_0)

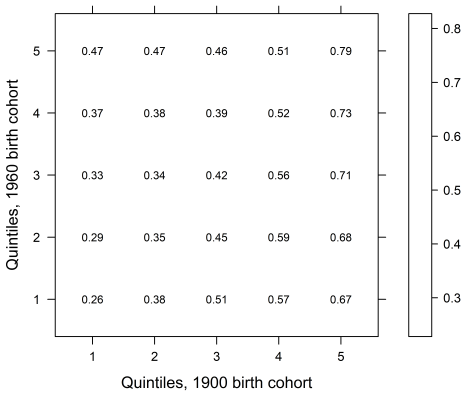

(c) Learning ability (ξ_h)

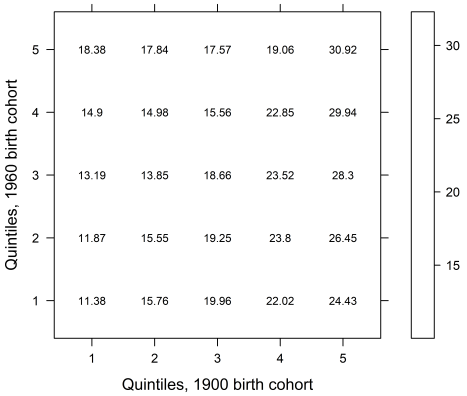

(d) Effort of schooling (ξ_e)

Figure 15: Distribution of the initial (unobservable) characteristics by wage quintile and birth cohort when the education-specific access to medical technology is shut down.

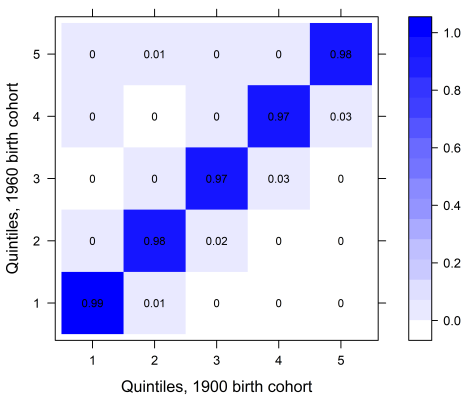

(a) Frequency

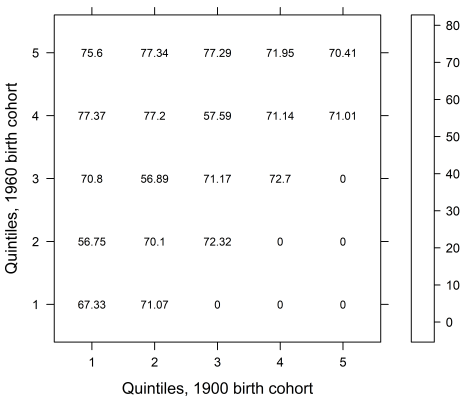

(b) Modal age at death (M_0)

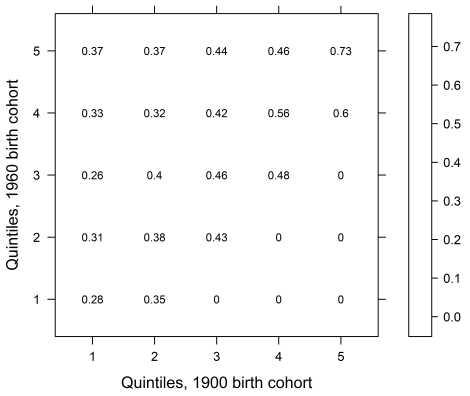

(c) Learning ability (ξ_h)

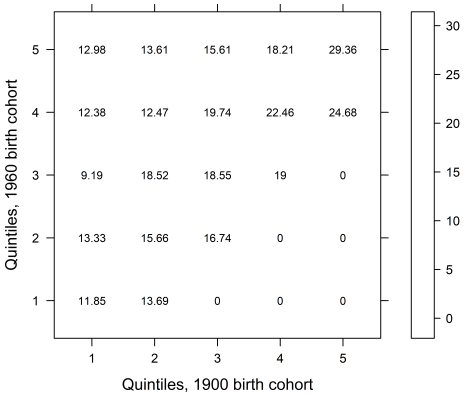

(d) Effort of schooling (ξ_e)

Figure 16: Distribution of the initial (unobservable) characteristics by wage quintile and birth cohort when the increase in wage rates is shut down.

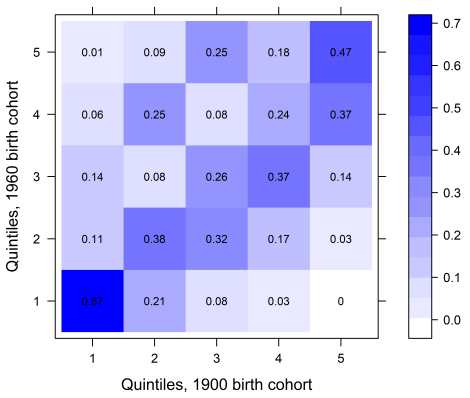

(a) Frequency

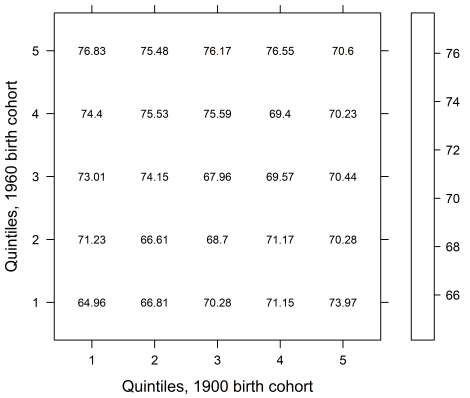

(b) Modal age at death (M_0)

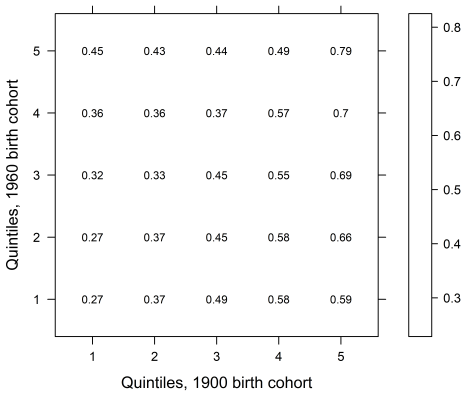

(c) Learning ability (ξ_h)

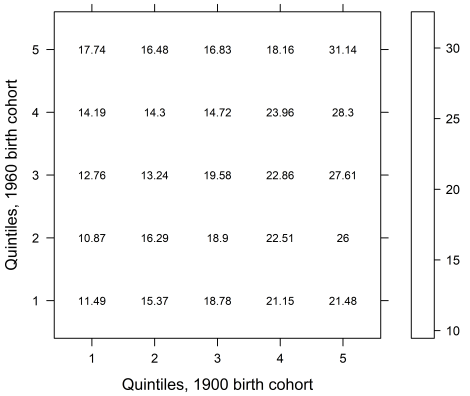

(d) Effort of schooling (ξ_e)

Figure 17: Distribution of the initial (unobservable) characteristics by wage quintile and birth cohort when the reduction in age-independent mortality is shut down.